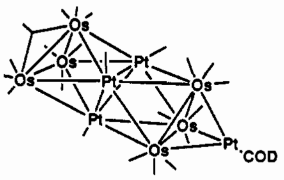

14

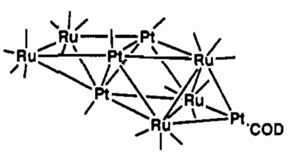

3

that cluster fragmentation is not as important a process in these reactions, although a significant amount of rearrangement of the metal–metal bonds is certainly required to transform the ladder structure of **1b** into the raft of **6**. This process is also readily reversible, since the treatment of **6** with CO at 25 °C regenerated **1b** in 40% yield in 5 min. Although the structure of **5** was not established crystallographically, it seems most likely that its structure is analogous to that of **6** with two carbonyl ligands on the platinum atom in the place of the COD ligand. The thermal decarbonylation of **6** leading to the formation of the closed-cluster complex **8** is similar to the cluster-closing transformations of $Os_6(CO)_{21}$ to $Os_6(CO)_{18}$[22,23] and $Os_5(CO)_{19}$ to $Os_5(CO)_{16}$[24] and is a natural consequence of decreased ligation.

The redox behavior of **5** and **6** is similar to that exhibited by $Pt_3Fe_3(CO)_{15}$[3,16] and a variety of phosphine and phosphite analogues of **11**.[23] The additional electrons in the anions of $[Pt_3Fe_3(CO)_{15}]^{n-}$ (n = 1,2) were proposed to occupy a low-lying in-plane antibonding orbital of A_2' symmetry that was concentrated principally on the three platinum atoms of the inner triangle.[16,25] The similar redox behavior of **5** supports its formulation as a raft type structure.

Acknowledgment. These studies were supported by the National Science Foundation under Grant No. CHE-8919786. We thank Dr. John Dawson for the use of his electrochemical equipment.

Supplementary Material Available: Tables of hydrogen atom and selected carbon atom positional parameters, anisotropic thermal parameters, and bond angles (17 pages); listings of structure factor amplitudes (56 pages). Ordering information is given on any current masthead page.

---

(22) Nicholls, J. N.; Farrar, D. H.; Jackson, P. F.; Johnson, B. F. G.; Lewis, J. *J. Chem. Soc., Dalton Trans.* **1982**, 1395.

(23) Goudsmit, R. J.; Jeffrey, J. G.; Johnson, B. F. G.; Lewis, J.; McQueen, R. C. S.; Sanders, A. J.; Liu, J.-C. *J. Chem. Soc., Chem. Commun.* **1986**, 24.

(24) Farrar, D. H.; Johnson, B. F. G.; Lewis, J.; Raithby, P.; Rosales, M. J. *J. Chem. Soc., Dalton Trans.* **1982**, 2051.

(25) Evans, D. G.; Mingos, D. M. P. *Organometallics* **1983**, *2*, 435.

Contribution from Department of Chemistry, 6-331,
Massachusetts Institute of Technology, Cambridge, Massachusetts 02139

Bimetallic Hydrazido(3– and 4–) and Nitrido Complexes of Tungsten Containing the $W(\eta^5\text{-}C_5Me_5)Me_3$ Core

Timothy E. Glassman, Andrew H. Liu, and Richard R. Schrock*

Received May 29, 1991

$Cp^*Me_3W{=}NNH_2$ (**1**) is successively deprotonated by Li-*n*-Bu to yield $[Cp^*Me_3W{=}NNHLi]_x$ (**2**) and then $[Cp^*Me_3W{=}NNLi_2]_x$ (**3**). Water reacts with **2** or **3** to re-form **1**. $SiMe_3Cl$ reacts with **2** or **3** to give $Cp^*Me_3W{=}NNH(SiMe_3)$ or $Cp^*Me_3W{=}NN(SiMe_3)_2$, respectively. Reaction of 0.5 equiv of $MgNp_2(TMEDA)$ with **1** yields $[Cp^*Me_3W{=}NNH]_2[\mu\text{-}Mg(TMEDA)]$, which can be recrystallized from THF to yield structurally characterized $[Cp^*Me_3W{=}NNH]_2[\mu\text{-}Mg(THF)_4]$ (**6**-$(THF)_4$; space group $P2_1/n$ (No. 14), a = 12.380 (6) Å, b = 15.252 (6) Å, c = 30.618 (8) Å, β = 97.91 (3)°, V = 5726 (7) Å^3, MW = 1099.14, ρ(calcd) = 1.275 g/cm^3, Z = 4, R = 0.082, R_w = 0.132). $Cp^*Me_3W{=}NNH\{MgNp(TMEDA)]$ (**7**) is obtained upon treating **1** with 1 equiv of $MgNp_2(TMEDA)$ at –40 °C; warming **7** to room temperature yields $[Cp^*Me_3W{=}NN]_2[\mu\text{-}Mg(TMEDA)]_2$ (**8**). $Cp^*Me_3W{=}N{-}N{=}TaCp^*Me_2$ (**9**) has been prepared by treating Cp^*TaMe_3Cl with **6** or Cp^*TaMe_4 with **1**. Complexes of the type $Cp^*Me_3W{=}NNH(ZrCp_2R)$ (R = Me (**10a**), CH_2Ph (**10b**)) are the products of the reactions between **1** and Cp_2ZrR_2, but they do not readily eliminate methane or toluene to generate a hydrazido(4–) complex. **10a** and **10b** react slowly with **1** to form $[Cp^*Me_3W{=}NNH]_2ZrCp_2$ (**11**). The tantalum and zirconium complexes react readily with water to re-form **1**. Reaction of $[Cp^*Me_3W{=}NLi]_x$ (**12**) with $Cp^*WMe_3(OTf)$ yields the symmetric, mixed-valent bridging nitride $[Cp^*Me_3W]_2(\mu\text{-}N)$ (**13a**), which has been characterized crystallographically (space group $P2_1/c$ (No. 14), a = 8.390 (4) Å, b = 20.341 (6) Å, c = 8.733 (4) Å, β = 117.83 (2)°, V = 1318 (2) Å^3, MW = 742.37, ρ(calcd) = 1.870 g/cm^3, Z = 2, R = 0.057, R_w = 0.063). The geometry about the tungsten in **13a** is square pyramidal, a center of inversion defines a linear W–N–W backbone that has a W–N distance of 1.8475 (8) Å. **13a** can be oxidized to yield $\{[Cp^*Me_3W]_2(\mu\text{-}N)\}^+$ (**13b**). **12** also reacts with Cp^*TaMe_3X (X = Cl, OTf) or $Cp^*TaMe_2(OTf)_2$ to give the unsymmetrical "metalloimido" complex $Cp^*Me_3W{\equiv}N\text{-}TaCp^*Me_3$ (**15**) or the bridging nitride $Cp^*Me_3W{=}N{=}TaCp^*Me_2(OTf)$ (**14**), respectively.

Introduction

Dinitrogen is activated by a variety of early transition metals (e.g., those in $Ti(OEt)_4$, $(\eta^5\text{-}C_5H_5)_2ZrCl_2$, $VCl_3(THF)_3$, and WCl_6) that have been reduced by sodium, lithium, magnesium, metal hydrides, or metal alkyls.[1] Mechanisms have been proposed that involve lithiated or magnesiated hydrazido and imido intermediates specifically.[2,3] Proposals for the activation of dinitrogen that involve two or more transition-metal centers are also common.[4–6] Typical multimetallic hydrazido species that have been proposed include trimetallic hydrazido(4–) derivatives (A), bimetallic hydrazido(3–) derivatives (B), and bimetallic hydrazido(4–) derivatives (C). Once the N–N bond has been cleaved, species that contain only one nitrogen atom bound between two or more metals (e.g., bridging nitrides, metalloimides, etc.) are proposed to be formed in such systems.

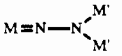

$M{\equiv}N{-}N(M')_2$

A

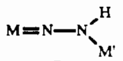

$M{\equiv}N{-}N(H)M'$

B

$M{\equiv}N{-}N{\equiv}M'$

C

We have been exploring the role of relatively high oxidation state (d^0–d^2) complexes in activating and reducing molecular nitrogen. Most recently, several hydrazido(4–) derivatives of the

---

(1) *New Trends in the Chemistry of Nitrogen Fixation*; Chatt, J., da Camara Pina, L. M., Richards, R. L., Eds.; Academic Press: New York, 1980.

(2) Shilov, A. E. *Russ. Chem. Rev.* (*Engl. Transl.*) **1974**, *43*, 378 and references therein.

(3) Yamamoto, A.; Miura, Y.; Ito, T.; Chen, H.-L.; Iri, K.; Ozawa, F.; Miki, K.; Sei, T.; Tanaka, N.; Kasai, N. *Organometallics* **1983**, *2*, 1429.

(4) Chatt, J.; Dilworth, J. R.; Richards, R. L. *Chem. Rev.* **1978**, *78*, 589 and references therein.

(5) Leigh, G. J. *J. Mol. Catal.* **1988**, *47*, 363.

(6) Leigh, G. J. *Transition Met. Chem.* (*London*) **1986**, *11*, 118.

Table I. ^{15}N NMR Data for a Series of Tungsten Hydrazido, Imido, and Nitrido Complexes[a]

compd		$\delta(N_\alpha)$	$\delta(N_\beta)$	$^1J_{N_\alpha W}$	$^2J_{N_\beta W}$	$^1J_{NN}$	$^1J_{N_\beta H}$	$^2J_{N_\alpha H}$
$Cp^*Me_3W{=}NNH_2$[b]	**1**	382.0	131.6[i]	129	14[c]	10.5	77	2
$[Cp^*Me_3W{=}NNHLi]_x$	**2**	445.6	211.9[i]	112	9	15.5	54	6
$[Cp^*Me_3W{=}NNLi_2]_x$ (45 °C)	**3**	418.7 (73)	312.2 (52)	no	no	no		
$[Cp^*Me_3W{=}NNLi_2]_y$ (−80 °C)	**3′**	434.9	362.2 (55)	86	no	15		
$[Cp^*Me_3W{=}NNH]_2[\mu\text{-}Mg(THF)_4]$	**6**-$(THF)_4$	425.9 (48)	192.2 (48)[i]	no	no	no	59	no
$[Cp^*Me_3W{=}NN]_2[\mu\text{-}Mg(TMEDA)]_2$	**8**	440.3	243.8	no	no	14		
$Cp^*Me_3W{=}NNH(SiMe_3)$[d]		375.6	147.1[i]	no	16.5	10.5	82	1
$Cp^*Me_3W{=}NN(SiMe_3)_2$[d]		368.6	161.6	131	no	12		
$Cp^*Me_3W{=}N{-}N{=}TaCp^*Me_2$[e]	**9**	429.7	370.0	117	13	11		
$Cp^*Me_3W{=}NNH(ZrCp_2Me)$	**10a**	403.0	259.5[i]	124	14.5	12	70	3
$[Cp^*Me_3W{=}NNH]_2ZrCp_2$	**11**	409.3	246.2[i]	125	14	12	71	3
$[Cp^*Me_3W{=}NLi]_x$	**12**	678.5		54				
$[Cp^*Me_3W{=}NLi]_x$[d]	**12**	624.6 (54)		no				
$[Cp^*Me_3W{=}N{=}WCp^*Me_3]^+$[f]	**13b**	634.9		63				
$Cp^*Me_3W{=}N{=}TaCp^*Me_2(OTf)$[e]	**14**	620.9		68				
$Cp^*Me_3W{=}N{-}N{=}WCp^*Me_3$[e,g]		428.7	428.7	125	104			
$Cp^*Me_3W{=}N{-}N{=}WCp^*Me_2(OTf)$[e]		423.6	410.0	111	17.5	9.5		
$Cp^*Me_2(OTf)W{=}N{-}N{=}WCp^*Me_2(OTf)$[e,g]		403.3	403.3	no	no			
$Cp^*Me_3W{=}N{-}N{=}MoCp^*Me_3$[e,h]		436.3	435.3	no	no	9		

[a] Spectra were recorded in THF-d_8 unless otherwise noted; chemical shifts are in ppm downfield of liquid ammonia (0 ppm) and are referenced to aniline-^{15}N (56.5 ppm); coupling constants are in hz as are line widths (in parentheses); no = not observed. [b] See ref 10. [c] Originally reported as <5 Hz.[b] [d] C_6D_6. [e] CD_2Cl_2. [f] CD_3NO_2. [g] See ref 7. [h] See ref 8. [i] Peak inverted due to negative NOE from adjacent hydrogen.

type $Cp^*Me_3M{=}N{-}N{=}M'Cp^*Me_3$ (M, M′ = Mo, W) have been synthesized and structurally characterized; their reduction in the presence of protons yields up to 1.85 equiv of ammonia.[7,8] In this paper, we turn to the study of bimetallic complexes that contain main-group or electropositive transition metals at one end of the N_2 ligand in order to test the possibilities that *hetero*bimetallic activation of the N_2 system might be more efficient and that the N_2 ligand, therefore, could be reduced to ammonia more readily. We noted in an earlier paper that $Cp^*Me_3W{=}NH$ is deprotonated by lithium reagents to give $[Cp^*Me_3W{=}NLi]_x$,[9] which has prompted us here to more thoroughly evaluate the nature of $[Cp^*Me_3W{=}NLi]_x$ and to synthesize other complexes that contain a single nitrogen atom between two metals.

Results

Lithium and Magnesium Derivatives of $Cp^*Me_3W{=}NNH_2$. *n*-Butyllithium successively deprotonates $Cp^*Me_3W{=}NNH_2$ (**1**)[10] to yield $[Cp^*Me_3W{=}NNHLi]_x$ (**2**) and then $[Cp^*Me_3W{=}NNLi_2]_x$ (**3**, eq 1). **2** is very soluble in diethyl ether, while **3** is

$$\underset{1}{Cp^*Me_3W{=}NNH_2} \xrightarrow[-n\text{-BuH}]{n\text{-BuLi}} \underset{2}{[Cp^*Me_3W{=}NNHLi]_x} \xrightarrow[-n\text{-BuH}]{n\text{-BuLi}} \underset{3}{[Cp^*Me_3W{=}NNLi_2]_x} \quad (1)$$

soluble only in aromatic or polar solvents; no solvent of coordination is observed in the NMR spectra of either. These solubility characteristics imply limited aggregation in **2** and more extensive aggregation in **3**, in each case resulting from N→Li interactions.[11] The ^{15}N NMR spectrum of **2** in THF-d_8 reveals a resonance for N_α at 445.6 ppm ($^1J_{NW}$ = 112 Hz) and one for N_β at 211.9 ppm ($^2J_{NW}$ = 9 Hz; see Table I). Proton, ^7Li, and ^{15}N NMR studies of **3** in THF-d_8 reveal a reversible, temperature-dependent equilibrium between two species (Figure 1). At 45 °C the ^{15}N NMR spectrum of **3** reveals a resonance for N_α at 418.7 ppm ($\Delta\nu_{1/2}$ = 73 Hz) and a resonance for N_β at 312.2 ppm ($\Delta\nu_{1/2}$ = 52 Hz), the breadths of which suggest that the nitrogens are coupled to lithium (^7Li, 92.6% abundant, $I = {}^3/_2$; ^6Li, 7.4% abundant, $I = 1$). At −80 °C a new N_α resonance, assigned to $[Cp^*Me_3W{=}NNLi_2]_y$ ($y < x$), is observed at 434.9 ppm and is much better resolved than the N_β resonance at 362.2 ppm ($\Delta\nu_{1/2}$ = 55 Hz). The value of $^1J_{NW}$ (86 Hz) is somewhat smaller than the 120-Hz coupling observed for tungsten–imido triple bonds, and $^1J_{NN}$ (15 Hz) is somewhat larger than the 10-Hz coupling found for most N–N bonds. Attempts to isolate a well-defined solvated complex of **3** employing chelating ligands such as $Me_2NCH_2CH_2NMe_2$ (TMEDA), $(H_2NCH_2CH_2)_2NH$, or 18-crown-6 were unsuccessful. The extreme air sensitivity of **3** as well as its insolubility in noncoordinating solvents and instability in coordinating solvents over periods of days has hampered attempts at molecular weight determination.

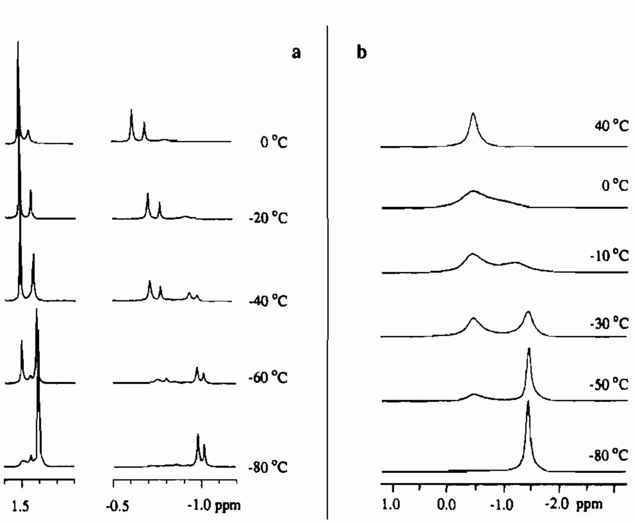

Figure 1. Variable-temperature (a) ^1H and (b) ^7Li NMR spectra of $[Cp^*Me_3W{=}NNLi_2]_x$ (**3**).

Both **2** and **3** react immediately with water to regenerate **1**, which is relatively stable to further hydrolysis. Trimethylchlorosilane also reacts with **2** and **3** to yield $Cp^*Me_3W{=}NNH(SiMe_3)$ and $Cp^*Me_3W{=}NN(SiMe_3)_2$, respectively (see Table I for ^{15}N NMR data). A number of other substituted derivatives of $Cp^*Me_3W{=}NNH_2$ have been prepared, many from substituted hydrazines.[12] (Other trimethylsilyl-substituted diazenido and hydrazido(2−) ligands have been reported.[13-15]) Attempted alkylations with alkyl halides (e.g., MeI, CH_2Cl_2, and *t*-$BuCH_2Cl$) were unsuccessful, although MeOTf (OTf = OSO_2CF_3) will alkylate **3** to yield traces of $[Cp^*Me_3W{=}$

---

(7) O'Regan, M. B.; Liu, A. H.; Finch, W. C.; Schrock, R. R.; Davis, W. M. *J. Am. Chem. Soc.* **1990**, *112*, 4331.

(8) Schrock, R. R.; Kolodziej, R. M.; Liu, A. H.; Davis, W. M.; Vale, M. G. *J. Am. Chem. Soc.* **1990**, *112*, 4338.

(9) Glassman, T. E.; Vale, M. G.; Schrock, R. R. *Organometallics*, in press.

(10) Schrock, R. R.; Liu, A. H.; O'Regan, M. B.; Finch, W. C.; Payack, J. F. *Inorg. Chem.* **1988**, *27*, 3574.

(11) For example: Reed, D.; Barr, D.; Mulvey, R. E.; Snaith, R. *J. Chem. Soc., Dalton Trans.* **1986**, 557 and references therein.

(12) Glassman, T. E.; Schrock, R. R. In preparation.

(13) Hidai, M.; Komori, K.; Komada, T.; Jin, D.-M.; Takahashi, T.; Sugiura, S.; Uchida, Y.; Mizobe, Y. *J. Organomet. Chem.* **1984**, 155.

(14) Wiberg, N.; Häring, H.-W.; Schubert, U. *Z. Naturforsch.* **1978**, *33B*, 1365.

(15) Wiberg, N. Häring, H.-W.; Huttner, G.; Friedrich, P. *Chem. Ber.* **1978**, *111*, 2708.

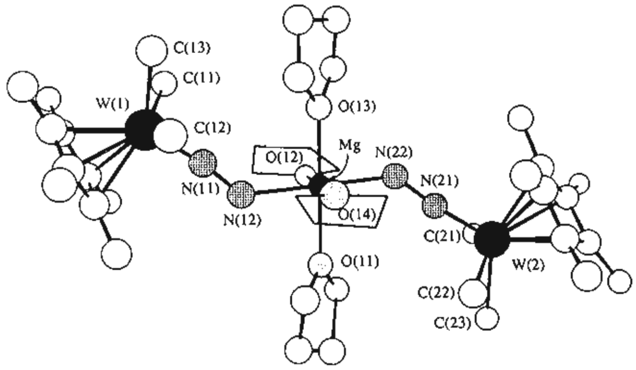

Figure 2. View of the X-ray crystal structure of $[Cp^*Me_3W{=}NNH]_2[\mu\text{-}Mg(THF)_4]$ (**6**-(THF)$_4$). Two of the coordinating THF ligands are outlined for clarity.

$NNMe_3]OTf$ (**4**). The reaction between $Cp^*Me_3W{=}NNMe_2$ and MeOTf generates **4** in much better yield,[12] suggesting that a proton will preferentially attack $Cp^*Me_3W{=}NNH_2$ at the terminal nitrogen.[10]

The reaction between $Cp^*Me_3W{=}NNH_2$ (**1**) and MgNpCl (Np = CH_2-*t*-Bu) at −40 °C in ether proceeds to form $[Cp^*MeW{=}NNH(MgCl)]_x$ (**5**, eq 2). Other magnesium reagents result in lower yields ($MeMgBr/Et_2O$), or the reaction is complicated by the strongly coordinating solvent (MeMgCl/THF; see below). Use of an excess of MgNpCl does not remove the second hydrazido proton; it only reduces the yield of **5**. **5** is a yellow powder that dissolves in polar solvents such as tetrahydrofuran, dimethoxyethane, or pyridine to yield yellow, crystalline $[Cp^*Me_3W{=}NNH]_2[\mu\text{-}Mg(S)_n]$ (**6**-S$_n$; eq 3). Four equivalents of THF or pyridine, or 1 equiv of the bulkier DME, binds to the magnesium in **6**-S$_n$ according to the proton NMR spectra. We did not find conditions that readily allowed separation of **6**-S$_n$ from $MgCl_2$; however, **6**-TMEDA can be prepared from **1** and 0.5 equiv of $MgNp_2(TMEDA)$ (eq 4). Recrystallization of **6**-TMEDA from a THF/pentane solution yields **6**-(THF)$_4$ in high yield; however, two of the four THF ligands are lost readily and the crystals degrade upon exposure to vacuum or washing with pentane. As one would expect, **6**-(py)$_4$, prepared in an analogous fashion, is more stable than **6**-(THF)$_4$ toward solvent loss. The ^{15}N NMR spectrum of **6**-(THF)$_4$ shows a fairly broad resonance for N_α at 425.9 ppm ($\Delta\nu_{1/2}$ = 48 Hz) as well as for N_β at 192.2 ppm ($\Delta\nu_{1/2}$ = 48 Hz). This broadening may be due to an equilibrium between the different solvated species. The overall structure of **6**-(THF)$_4$ was determined in a single-crystal X-ray diffraction study (Figure 2), but due to crystal degradation, the data did not refine well (see supplementary material). The two square-pyramidal tungsten centers are connected through a near-linear W=N—N linkage to trans positions on magnesium in an octahedral coordination sphere. The four THF molecules occupy equatorial positions around magnesium, a feature noted in the closely related structure of $[(PR_3)_3CoNN]_2[\mu\text{-}Mg(THF)_4]$.[3,16] The hydrazido proton is probably in the WNNMg plane, which is perpendicular to the Cp* plane. We assume that the structures of the examples of **6** in which the coordination geometry about magnesium is tetrahedral are similar to that of **6**-(THF)$_4$.

$$\underset{\mathbf{1}}{Cp^*WMe_3(NNH_2)} \xrightarrow[-CMe_4]{MgNpCl} \underset{\mathbf{5}}{[Cp^*Me_3W{=}NNH(MgCl)]_x} \tag{2}$$

$$2\ \underset{\mathbf{5}}{[Cp^*Me_3W{=}NNH(MgCl)]_x} \xrightarrow{S} \underset{\mathbf{6\text{-}S_n}}{[Cp^*Me_3W{=}NNH]_2[\mu\text{-}Mg(S)_n]} + MgCl_2 \tag{3}$$

(S = THF, DME, pyridine)

$$2\ \underset{\mathbf{1}}{Cp^*WMe_3(NNH_2)} \xrightarrow[-2\,CMe_4]{MgNp_2(TMEDA)} \mathbf{6}\text{-TMEDA} \tag{4}$$

Scheme I

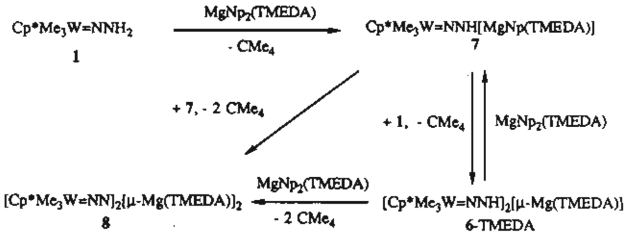

It is possible to remove both hydrazido(2−) protons from **1** by adding 1 equiv of $MgNp_2(TMEDA)$ at room temperature to give red, crystalline $[Cp^*Me_3W{=}NN]_2[\mu\text{-}Mg(TMEDA)]_2$ (**8**) in 60% yield (eq 5). If the reaction is performed at −40 °C, then intermediate yellow, crystalline $Cp^*Me_3W{=}NNH[MgNp(TMEDA)]$ (**7**; Scheme I) can be isolated. As one might expect, **7** reacts with **1** to give **6**-TMEDA (Scheme I). Warming a solution of **7** to room temperature yields **8** and neopentane. No THF analogue of **8** could be isolated. According to proton NMR spectra, TMEDA is displaced when **8** is dissolved in THF, but subsequent removal of solvent results in decomposition. Two plausible pathways for the formation of **8** are shown in Scheme I. The reaction between **6**-TMEDA and $MgNp_2(TMEDA)$ yields **8**; however, **7** is also observed, making it difficult to say whether bimolecular reaction of **7** is actually generating **8**. The structure of $[Cp^*Me_3W{=}NN]_2[\mu\text{-}Mg(TMEDA)]_2$ (**8**) is proposed to be similar to the structurally characterized analogues $[(PMe_3)_3CoNN]_2[\mu\text{-}Mg(OEt_2)t\text{-}Bu)]_2$,[17] $[(PMe_3)_3CoNN]_2(\mu\text{-}AlMe_2)_2$,[18] and $[(PMe_2Ph)_3(py)ClWNN]_2(\mu\text{-}AlCl_2)_2$.[19]

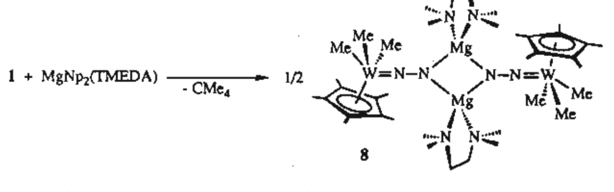

(5)

Attempts to analyze the lithium- and magnesium-substituted compounds for C, H, and N have produced variable and unsatisfactory results, due in part perhaps to their extreme oxygen sensitivity. Exposure to oxygen results in formation of an unknown paramagnetic species that is a brilliant shade of green-blue (λ_{max} = 594 nm) in solution which slowly fades to pale yellow over a 15-min period.

As with the lithium derivatives, hydrolysis of **6**, **7**, and **8** yields **1**, and reaction with trimethylchlorosilane yields $Cp^*Me_3W{=}NNH(SiMe_3)$ or $Cp^*Me_3W{=}NN(SiMe_3)_2$. Other alkylations (e.g., MeI) thus far have not yielded any products analogous to the trimethylsilyl derivatives.

Heterobimetallic Transition-Metal Derivatives. The hydrazido(4−) species $Cp^*Me_3W{=}N{-}N{=}MCp^*Me_3$ (M = W, Mo) have been prepared by treating $Cp^*Me_3W{=}NNH_2$ (**1**) with $[Cp^*WMe_4]PF_6$[7] or $[Cp^*MoMe_3(OAr)]PF_6$ (OAr = O-2,6-$Me_2C_6H_3$),[8] respectively. An alternate, albeit low-yield, synthesis of these complexes utilizes $[Cp^*Me_3W{=}NNH]_2[\mu\text{-}Mg(TMEDA)]$ (**6**-TMEDA; eqs 6 and 7). The hydrazido(3−) complexes $Cp^*Me_3W{=}NNH(MCp^*Me_3X)$ (M = W, X = Me; M = Mo, X = OAr) are probable intermediates, from which loss of methane

$$\text{6-TMEDA} + 2\ [Cp^*WMe_4]PF_6 \xrightarrow{-CH_4} Cp^*Me_3W{=}N{-}N{=}WCp^*Me_3 \tag{6}$$

$$\text{6-TMEDA} + 2\ [Cp^*MoMe_3(OAr)]PF_6 \xrightarrow{-HOAr} Cp^*Me_3W{=}N{-}N{=}MoCp^*Me_3 \tag{7}$$

---

[16] Hammer, R.; Klein, H.-F.; Schubert, U.; Frank, A.; Huttner, G. *Angew. Chem., Int. Ed. Engl.* **1976**, *15*, 612.

[17] Klein, H.-F.; Konig, H.; Koppert, S.; Ellrich, K.; Riede, J. *Organometallics* **1987**, *6*, 1341.

[18] Klein, H.-F.; Ellrich, K.; Ackermann, K. *J. Chem. Soc., Chem. Commun.* **1983**, 888.

[19] Takahashi, T.; Kodama, T.; Watakabe, A.; Uchida, Y.; Hidai, M. *J. Am. Chem. Soc.* **1983**, *105*, 1680.

Scheme II

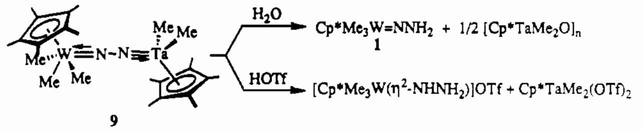

or phenol would afford the product.

In a related reaction, **6**-TMEDA reacts with Cp^*TaMe_3Cl[20] to form $Cp^*Me_3W{=}N{-}N{=}TaCp^*Me_2$ (**9**, eq 8). The reaction

$$\text{6-TMEDA} + 2\ Cp^*TaMe_3Cl \xrightarrow[\text{-MgCl}_2\text{(TMEDA)}]{-2\ CH_4} 2\ \underset{\mathbf{9}}{Cp^*Me_3W{=}N{-}N{=}TaCp^*Me_2} \qquad (8)$$

between **1** and Cp^*TaMe_4 also gives **9**, but more slowly; evidently, initial coordination of N_β of the hydrazido(2–) ligand to the less electrophilic tantalum center and elimination of the first equivalent of methane are relatively slow. Ammonia[21] and primary amines react much more readily with Cp^*TaMe_4. The most notable feature of the ^{15}N NMR spectrum of **9** [δ 429.7 ppm (WN, $^1J_{NW}$ = 117 Hz, $^1J_{NN}$ = 11 Hz) and 370.0 ppm (TaN, $^2J_{NW}$ = 13 Hz, $^1J_{NN}$ = 11 Hz)] is the small two-bond NW coupling (Table I). This value could be interpreted as evidence for limited delocalization throughout the W=N—N=Ta bond system, in contrast to $^2J_{NW}$ = 104 Hz in $[Cp^*Me_3W]_2(\mu\text{-}N_2)$.[7] The infrared spectrum of **9** in dichloromethane or as a thin film exhibits a strong absorption at 890 cm^{-1}, which shifts to 862 cm^{-1} in **9**-$^{15}N_2$, approximately what one would predict for a pure M–N stretch (Table III). (The similar masses of Ta and W probably result in a superposition of the Ta–N and W–N stretches.) Hydrolysis of **9** readily gives $Cp^*Me_3W{=}NNH_2$ (**1**) and insoluble $[Cp^*TaMe_2O]_n$[22] (Scheme II), in marked contrast to the unusual stability of $[Cp^*Me_3W]_2(\mu\text{-}N_2)$ toward hydrolysis. Addition of triflic acid to **9** yields $[Cp^*Me_3W(\eta^2\text{-}NHNH_2)]OTf$,[10] presumably by subsequent protonation of **1**, and $Cp^*TaMe_2(OTf)_2$, which can be independently prepared by addition of 2 equiv of triflic acid to Cp^*TaMe_4.

It is not possible to prepare "$Cp^*Me_3W{=}NN(TaCp^*Me_3)_2$" by treating $[Cp^*Me_3W{=}NNLi_2]_x$ (**3**) or $[Cp^*Me_3W{=}NN]_2[\mu\text{-}Mg(TMEDA)]_2$ (**8**) with excess Cp^*TaMe_3Cl. The reaction between **3** and Cp^*TaMe_3Cl forms $Cp^*Me_3W{=}N{-}N{=}TaCp^*Me_2$ (**9**), and presumably LiMe, which then alkylates a second equivalent of Cp^*TaMe_3Cl to form Cp^*TaMe_4 (eq 9).

$$\underset{\mathbf{3}}{[Cp^*Me_3W{=}NNLi_2]_x} + 2\ Cp^*TaMe_3Cl \xrightarrow{-2\ LiCl} \mathbf{9} + Cp^*TaMe_4 \qquad (9)$$

The reaction between 2 equiv of Cp^*TaMe_3Cl and **8** also yields **9**, but since MeMgCl is slower to alkylate Cp^*TaMe_3Cl, 1 equiv of Cp^*TaMe_3Cl remains.

Cp_2ZrR_2 (R = Me, CH_2Ph) reacts cleanly with $Cp^*Me_3W{=}NNH_2$ (**1**) overnight to yield bright orange $Cp^*Me_3W{=}NNH(ZrCp_2R)$ (**10a**, R = Me; **10b**, R = CH_2Ph; eq 10). Further

$$Cp_2ZrR_2 \xrightarrow[-RH]{\mathbf{1}} \underset{\substack{\mathbf{10a}:\ R = Me \\ \mathbf{10b}:\ R = CH_2Ph}}{Cp^*Me_3W{=}NNH(ZrCp_2R)} \xrightarrow[-RH]{\mathbf{1}} \underset{\mathbf{11}}{[Cp^*Me_3W{=}NNH]_2ZrCp_2} \qquad (10)$$

reaction of **10** with **1** slowly yields $[Cp^*Me_3W{=}NNH]_2ZrCp_2$ (**11**), which precipitates overnight in moderate yield if the reaction is performed in a *minimum* of ether. Both **10** and **11** are hydrolyzed readily to give **1** and $[Cp_2ZrMe]_2O$[23] and $[Cp_2ZrO]_3$,[24] respectively.

The resonances for the hydrazido proton in complexes **10** and **11** are found downfield of analogous resonances in Si, Mg, and Li derivatives (Table II). As for **9**, the relatively small values of $^2J_{NW} \approx 14$ Hz in **10** and **11** could be taken as evidence that there is little conjugation through the WNNZr backbone. The absence of any obvious N–H stretch in the infrared spectra of **10** and **11** suggests that the N–H vibration may be strongly coupled to another vibrational mode. A similar observation was made for $Cp^*WMe_3(\mu\text{-}NNH)WCp^*Me_2(\mu\text{-}NN)WCp^*Me_3$.[12] A perhaps less likely alternative involves a possible NH agostic interaction[25,26] with the metal.

The geometry of **10** is expected to be related to that of known amido complexes of group 4 metallocenes.[27-29] On the basis of equivalence of the Cp resonances in the proton NMR spectra of **10** in THF-d_8 down to –80 °C, the H–N–Zr plane cannot be oriented perpendicular to the N–Zr–R plane, an orientation that is required in order to form a dative Zr–N π bond. This observation is consistent with the bulk of this "amido" ligand. The Cp ligands may equilibrate by oscillation about the M–N bond, as observed in $Cp^*_2HfH(NHMe)$.[29] Trimetallic **11** may have a C_2 axis of symmetry, which would render the two amide groups equivalent.

It has been shown that PMe_3 traps the organometallic product following the loss of benzene from Cp_2ZrPh_2[30] and that THF traps intermediate "$Cp_2Zr(N\text{-}t\text{-}Bu)$" to give $Cp_2Zr(N\text{-}t\text{-}Bu)(THF)$.[31] However, attempts to eliminate methane or toluene by heating or photolyzing **10a** or **10b** in the presence of PMe_3 or THF led to decomposition rather than formation of the hypothetical "$Cp^*Me_3W{=}N{-}N{=}ZrCp_2(L)$". Further reaction between **10a** and **11** occurs slowly by *inter*molecular elimination of methane to form condensed, polymetallic species. For example, red crystals are formed whose proton NMR spectrum is consistent with that of a compound having three inequivalent WCp* ligands, four inequivalent ZrCp ligands, and seven inequivalent methyl groups. A plausible empirical formula is $Cp^*_3W_3Me_7Cp_4Zr_2N_x$, where x is either 4 or 6. We believe all of the methyl groups are attached to tungsten atoms. Heating **11** in THF-d_8 in a sealed NMR tube at 50 °C for 2 days yielded a dark red crystalline material that is insoluble in all common solvents. We speculate that this product is a related oligomer or polymer formed by repeated intermolecular elimination of methane.

The low values for $^2J_{WN}$ of 13–15 Hz in the W–Ta hydrazido(4–) complex **9** and the W–Zr hydrazido(3–) complexes **10** and **11** are comparable to the 14 Hz observed in $Cp^*WMe_3(NNH_2)$[12] rather than the 104 Hz observed in $[Cp^*Me_3W]_2(\mu\text{-}N_2)$ (Table I).[7] This suggests that the heterometallic systems possess more localized electronic structures similar to that in $Cp^*WMe_3(NNH_2)$, rather than to the extensively delocalized π system in $[Cp^*Me_3W]_2(\mu\text{-}N_2)$. Delocalization probably contributes to the resistance of the hydrazido(4–) complex to hydrolysis.[7] Cop-

Table II. ^1H NMR Data for Monosubstituted Tungsten Hydrazido(2–) Complexes[a]

compd		δ(NH), ppm
$Cp^*Me_3W{=}NNH_2$[b]	**1**	4.48
$Cp^*MeW{=}NNH(SiMe_3)$		5.12
$[Cp^*MeW{=}NNH(MgCl)]_x$	**5**	5.56
$[Cp^*Me_3W{=}NNH]_2[\mu\text{-}Mg(THF)_2]$	**6**	5.56
$Cp^*Me_3W{=}NNH[MgNp(TMEDA)]$	**7**	5.61
$[Cp^*Me_3W{=}NNHLi]_x$	**2**	6.10
$[Cp^*WMe_3NNH]_2ZrCp_2$	**11**	7.81
$Cp^*Me_3W{=}NNH(ZrCp_2Me)$	**10a**	8.03
$Cp^*Me_3W{=}NNH(ZrCp_2CH_2Ph)$	**10b**	8.11

[a] Spectra acquired at ca. 20 °C in C_6D_6. [b] See ref 10.

---

(20) Wood, C. D.; Schrock, R. R. *J. Am. Chem. Soc.* **1979**, *101*, 5421.

(21) Banaszak Holl, M. M.; Kersting, M.; Pendley, B. D.; Wolczanski, P. T. *Inorg. Chem.* **1990**, *29*, 1518.

(22) For related complexes: Jernakoff, P.; de Meric de Bellefon, C.; Geoffroy, G. L.; Rheingold, A. L.; Geib, S. J. *Organometallics* **1987**, *6*, 1362.

(23) Hunter, W. E.; Hrncir, D. C.; Vann Bynum, R.; Penttila, R. A.; Atwood, J. L. *Organometallics* **1983**, *2*, 751.

(24) Fachinetti, G.; Floriani, C.; Chiesi-Villa, A.; Guastini, C. *J. Am. Chem. Soc.* **1979**, *101*, 1767.

(25) Brookhart, M.; Green, M. L. H. *J. Organomet. Chem.* **1983**, *250*, 395.

(26) Brookhart, M.; Green, M. L. H.; Wong, L.-L. *Prog. Inorg. Chem.* **1988**, *36*, 1.

(27) Hillhouse, G. L.; Bercaw, J. E. *Organometallics* **1982**, *1*, 1025.

(28) Hillhouse, G. L.; Bulls, A. R.; Santarsiero, B. D.; Bercaw, J. E. *Organometallics* **1988**, *7*, 1309.

(29) Hillhouse, G. L.; Bercaw, J. E. *J. Am. Chem. Soc.* **1984**, *106*, 5472.

(30) Buchwald, S. L.; Watson, B. T. *J. Am. Chem. Soc.* **1986**, *108*, 7411.

(31) Walsh, P. J.; Hollander, F. J.; Bergman, R. G. *J. Am. Chem. Soc.* **1988**, *110*, 8729.

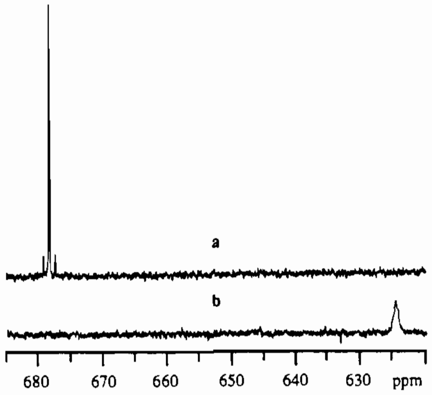

Figure 3. ^{15}N NMR spectra of $[Cp^*Me_3W{=}^{15}NLi]_x$ (**12**) in (a) THF-d_8 and (b) C_6D_6.

per-colored $Cp^*Me_3W{=}N{-}N{=}WCp^*Me_2(OTf)$ was prepared by addition of 1 equiv of triflic acid to $[Cp^*Me_3W]_2(\mu\text{-}N_2)$ in order to test whether a perturbation of the WNNW system would affect the electron delocalization across the backbone. Triflate absorptions at 1197, 1010, and 617 cm^{-1} in the IR spectrum suggest that the triflate is bound to the metal, as presumably is the case in $Cp^*WMe_3(OTf)$, which has corresponding absorptions at 1192, 1006, and 632 cm^{-1} (cf. free triflate ion absorptions at 1258, 1030, and 637 cm^{-1}, respectively). The ^{15}N NMR spectrum of $Cp^*Me_3W{=}^{15}N_\alpha{-}^{15}N_\beta{=}WCp^*Me_2(OTf)$ has resonances for N_α at 423.6 ppm ($^1J_{N_\alpha W}$ = 111 Hz, $^2J_{N_\beta W}$ = 17.5 Hz) and for N_β at 410.0 ppm ($^1J_{N_\beta W}$ and $^2J_{N_\alpha W}$ were not resolved). The chemical shifts are intermediate between the values reported for $[Cp^*Me_3W]_2(\mu\text{-}N_2)$ and $[Cp^*Me_2(OTf)W]_2(\mu\text{-}N_2)$ (Table I).[7] The one-bond WN coupling is similar to that observed in $[Cp^*Me_3W]_2(\mu\text{-}N_2)$. On the other hand, the two-bond coupling is significantly smaller, implying a disruption of the WNNW delocalization. Apparently, the W=N—N=W system in $[Cp^*Me_3W]_2(\mu\text{-}N_2)$ does enjoy a special stability as a result of π delocalization.

Bridging-Nitrido Complexes. In a previous paper devoted to amino, amido, and imido complexes containing the Cp^*Me_3M core, we noted that decomposition of $[Cp^*WMe_3(NH_2)]PF_6$ produced deep red $\{[Cp^*Me_3W]_2(\mu\text{-}N)\}PF_6$ (**13b**) in variable yields (eq 11), while generation of $[Cp^*WMe_3(NH_2)]PF_6$ in the presence of a base gave $Cp^*Me_3W{=}NH$ quantitatively.[9] The low-field resonance in the ^{15}N NMR spectrum of **13b** at 634.9 ppm is consistent with a positively charged, multiply bonded "nitride" or iminium-like nitrogen atom, as is $^1J_{NW}$ = 63 Hz, which in this class of compounds is intermediate between a typical value found for an imido group ($^1J_{NW}$ = 115 Hz) and that for an amido group ($^1J_{NW}$ < 5 Hz). The ^{183}W satellites constitute 28% of the peak intensity in **13b**, verifying the W=N=W connectivity.

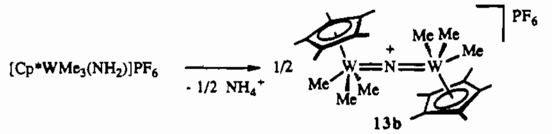

13b

(11)

Before a description of an alternative, higher yield route to **13b** that employs $[Cp^*Me_3W{=}NLi]_x$ (**12**), which was prepared by addition of *n*-butyllithium to $Cp^*Me_3W{=}NH$,[9] multinuclear NMR studies that elucidate the nature of **12** in solution will be discussed. The ^{15}N NMR spectrum of **12** in THF-d_8 (or pyridine-d_5) contains a sharp singlet at 679 ppm ($^1J_{NW}$ = 54 Hz); in contrast, a broad resonance is observed in C_6D_6 at 624.6 ppm ($\Delta\nu_{1/2}$ = 54 Hz; Figure 3). These data are in accord with solvation of the lithium by THF or pyridine, perhaps even to give a monomeric $Cp^*Me_3W{=}NLi(S)_n$ species, or a rapid equilibrium between a solvated species and one of higher nuclearity. The breadth of the resonance in benzene could be explained if one or more aggregates of **12** of varying size *x* were present. Most likely, a single aggregate is present in which the nitrogen is in a relatively unsymmetric environment and therefore coupled extensively to the adjacent ^7Li quadrupole. Examination of **12**-^{15}N using natural-abundance ^6Li NMR spectroscopy is more informative because the magnitude of the electric quadrupolar moment for ^6Li is much smaller than it is for ^7Li[32] and the line widths are consequently narrower and coupling to ^{15}N is better resolved. In THF-d_8 a sharp singlet is observed with no discernible coupling between ^6Li and either ^{14}N or ^{15}N. In C_6D_6 the ^6Li resonance of **12** is a singlet for the ^{14}N isotopomer but is an apparent quartet ($^1J_{^6Li^{15}N}$ = 2.0 Hz) for the ^{15}N-labeled compound (Figure 4), consistent with each lithium being bound to *three* nearly equivalent nitrogen atoms.

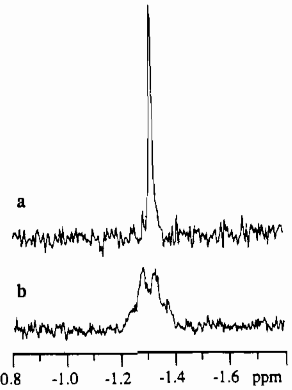

Figure 4. ^6Li NMR spectra of (a) $[Cp^*Me_3W{=}NLi]_x$ (**12**) and (b) **12**-^{15}N in C_6D_6.

The solvation and aggregation effects proposed above are analogous to those found for lithium amides $[Li(NR_2)]_x$ and imides $[Li(N{=}CR_2)]_x$, which have been studied extensively by ^6Li, ^7Li, ^{13}C, and ^{15}N NMR spectroscopy.[11,33,34] Lithium amides display a diverse array of structural types, most commonly dimeric (square) and trimeric (hexagonal) arrays of alternating Li and N in which typically $^1J_{^6Li^{15}N} \approx$ 3–6 Hz; the less sterically crowded lithium imides often adopt cubic $[LiN]_4$ (stacked squares) or prismatic $[LiN]_6$ (stacked six-membered rings in the chair conformation) structures based on alternating lithium–nitrogen frameworks.[35-38] In both the $[LiN]_4$ and $[LiN]_6$ imides, the lithium atoms are bound to three equivalent nitrogen nuclei. These tetrameric and hexameric compounds usually are soluble in benzene, in which they have been shown to retain their aggregation, and dissolve readily in coordinating solvents or in the presence of bases.[11] Although the finding that each nitrogen in $[Cp^*Me_3W{=}NLi]_x$ is bound to three lithium atoms is not surprising in view of the known structures of lithium imides, the presence of a four-coordinate nitrogen does require a lowering of the W–N bond order from that in a typical imide complex. Interestingly, the observed value of $^1J_{NW}$ = 54 Hz is *small* compared to a typical value for an imido nitrogen in complexes such as $Cp^*Me_3W{=}^{15}NH$ ($^1J_{NW}$ = 113 Hz)[9] and is comparable to that in $Cp^*Me_4W(NH_2)$ ($^1J_{NW}$ = 45 Hz).[9]

The postulated monomeric, solvated form and the more highly aggregated form of $[Cp^*Me_3W{=}NLi]_x$ (**12**) could closely resemble the structurally characterized complexes $(PR_3)_3CoNNLi(THF)_3$[3] and $[(PMe_3)_3CoNNK]_6$, respectively.[39,40]

---

(32) *CRC Handbook of Chemistry and Physics*, 63rd ed.; Weast, R. C., Astle, M. J., Eds.; CRC Press: Boca Raton, FL, 1982; p E-66.

(33) Faliano-Roth, A. S.; Michaelides, E. M.; Collum, D. B. *J. Am. Chem. Soc.* **1988**, *110*, 2658.

(34) Jackman, L. M.; Scarmoutzos, L. M.; Porter, W. *J. Am. Chem. Soc.* **1987**, *109*, 6524.

(35) Barr, D.; Clegg, W.; Mulvey, R. E.; Snaith, R.; Wade, K. *J. Chem. Soc., Chem. Commun.* **1986**, 295 and references therein.

(36) Setzer, W.; Schleyer, P. v. R. *Adv. Organomet. Chem.* **1985**, *24*, 353 and references therein.

(37) Armstrong, D. R.; Barr, D.; Clegg, W.; Mulvey, R. E.; Reed, D.; Snaith, R.; Wade, K. *J. Chem. Soc., Chem. Commun.* **1986**, 869.

(38) Barr, D.; Clegg, W.; Mulvey, R. E.; Snaith, R.; Wright, D. S. *J. Chem. Soc., Chem. Commun.* **1987**, 716.

(39) Hammer, R.; Klein, H.-F.; Friedrich, P.; Huttner, G. *Angew. Chem., Int. Ed. Engl.* **1977**, *7*, 485.

(40) Klein, H.-F.; Hammer, R.; Wenninger, J.; Friedrich, P.; Huttner, G. *Z. Naturforsch.* **1978**, *33B*, 1267.

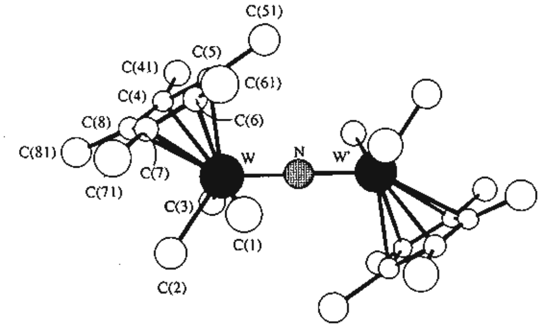

Figure 5. View of the X-ray crystal structure of $[Cp^*Me_3W]_2(\mu\text{-}N)$ (**13a**) (W–N = 1.8475 (8) Å, W–C(1) = 2.23 (2) Å, W–C(2) = 2.20 (2) Å, W–C(3) = 2.19 (2) Å, W–N–W = 180°, C(1)–W–C(3) = 138.4 (7)°, C(2)–W–N = 125.2 (6)°, C(2)–W–C(3) = 77.2 (9)°).

X-ray crystal structure studies of $[(PhLi)_3Ni]_2N_2(Et_2O)_2$[41] and $[Ph[Na{\cdot}OEt_2]_2(Ph_2Ni)_2N_2NaLi_6(OEt)_4{\cdot}Et_2O]_2$[42] show that the alkali metals either bridge the transition-metal–nitrogen bonds or cap a face composed of two transition metals and one nitrogen atom. Similar interactions may be involved in stabilizing $[Cp^*Me_3W{=}NNLi_2]_x$ (**3**) in the solid state and perhaps in solution.

A plausible method for formation of bridging-nitrido complexes is to employ $[Cp^*Me_3W{=}NLi]_x$ (**12**) in a nucleophilic displacement reaction. The reaction between **12** and $Cp^*WMe_3(OTf)$ yields the forest green, mixed-valent nitride $[Cp^*Me_3W]_2(\mu\text{-}N)$ (**13a**) (eq 12) in high yield. Oxidation of **13a** with $[FeCp_2]PF_6$ yields $\{[Cp^*Me_3W]_2(\mu\text{-}N)\}PF_6$ (**13b**) cleanly. Similar reactions in which (trimethylsilyl)imido complexes are "condensed" with metal halides to yield heterobimetallic[43] and polymeric[44] homometallic bridging nitride/metalloimides have been reported.

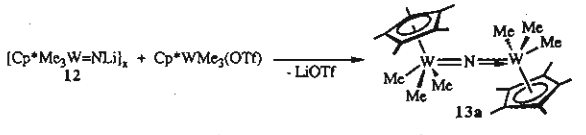

(12)

The poor solubility of **13a** in all common organic solvents is somewhat surprising, since the hydrazido(4–) analogue $[Cp^*Me_3W]_2(\mu\text{-}N_2)$ is soluble in diethyl ether and cationic **13b** readily dissolves in dichloromethane. The lack of any proton NMR signal for **13a** and observation of a broad ESR absorption at $\langle g \rangle = 1.916$ ($\Delta\nu_{1/2}$ = 119 G) support a delocalized, symmetric WNW core, a proposal that is confirmed in an X-ray diffraction study (Figure 5). Each metal center has a square-pyramidal geometry, and the molecule possesses a crystallographically imposed center of inversion. Therefore, the WNW backbone is linear and the W–N distances (1.8475 (8) Å) are equivalent. The W–N distance compares favorably with M–N distances in other group 6 symmetric, bridging-nitride complexes, $\{[Br_5Ta]_2(\mu\text{-}N)\}Br_3$ (1.849 (2) Å) and $\{[I_5Ta]_2(\mu\text{-}N)\}I_3$ (1.847 (6) Å)[45-47] and $[Mo\{S_2P(OMe)_2\}_2]_4(\mu\text{-}N)_4$ (1.87 (1) Å).[48] The most common type of bridging nitrides are largely the "asymmetric bridging nitride" (a) and the "metalloimide" (b). There are fewer "symmetric bridging nitrides" of types c and d. In addition to the symmetric, bridging-nitride complexes mentioned above, a number of others have also been reported.[49]

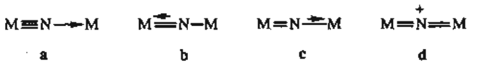

a b c d

Table III. Characteristic IR Absorptions for Bridging Nitride and Hydrazido(4–) Complexes[a]

compd		ν(WN)	$\nu(W^{15}N)$
$Cp^*Me_3W(\mu\text{-}N_2)WCp^*Me_3$[b]		889	861
$Cp^*Me_3W(\mu\text{-}N_2)WCp^*Me_2(OTf)$		883	
$Cp^*Me_3W(\mu\text{-}N_2)TaCp^*Me_3$	**9**	890	862
$Cp^*Me_3W(\mu\text{-}N)WCp^*Me_3$	**13a**	800	789
$[Cp^*Me_3W(\mu\text{-}N)WCp^*Me_3]PF_6$	**13b**	999	969
$Cp^*Me_3W(\mu\text{-}N)TaCp^*Me_2(OTf)$	**14**	1020, 981[c]	1012, 964[c]
$Cp^*Me_3W(\mu\text{-}N)TaCp^*Me_3$	**15**	1014	983

[a] Spectra acquired as Nujol mulls between KBr plates; frequencies in cm^{-1}. [b] See ref 7. [c] May be due to the OTf group.

Cyclic voltammetry studies of **13a** in dichloromethane reveal waves corresponding to a reversible redox couple ($\Delta(E_{pa} - E_{pc})$ = 78 mV) for $[Cp^*Me_3W]_2(\mu\text{-}N)^{0/+}$ at –0.736 V vs $FeCp_2^{0/+}$. The relatively negative potential for the **13a**/**13b** couple is good evidence that a delocalized π-bonding system involving W(VI) at each end is energetically favorable. The infrared spectrum of **13a** reveals an absorption that presumably is related to the WNW framework, which moves from 800 to 789 cm^{-1} upon labeling with ^{15}N; the low energy and small isotopic shift are unusual. An infrared absorption for $\{[Cp^*Me_3W]_2(\mu\text{-}N)\}PF_6$ (**13b**) shifts, upon ^{15}N labeling, from 999 to 969 cm^{-1} (Δ = 30 cm^{-1}; Table III), in accord with the expected shift of 31 cm^{-1} for a pure W–N mode.[9] This finding suggests that the absorption in $[Cp^*Me_3W]_2(\mu\text{-}N_2)$ that shifts from 889 to 861 cm^{-1} (Δ = 28 cm^{-1})[7] upon ^{15}N labeling also can be ascribed solely to a ν(WN) mode.

The reaction between $[Cp^*Me_3W{=}NLi]_x$ (**12**) and $Cp^*TaMe_2(OTf)_2$ yields dichloromethane-soluble, deep red $Cp^*Me_3W(\mu\text{-}N)TaCp^*Me_2(OTf)$ (**14**), which is readily alkylated to yield the bright orange, poorly soluble $Cp^*Me_3W(\mu\text{-}N)TaCp^*Me_3$ (**15**) (eq 13). Reaction of **12** with Cp^*TaMe_3X (X = Cl, OTf) yields **15** directly. The electronic structure of the WNTa backbone of these two related compounds is believed to be quite different. The ^{15}N NMR spectrum of **14** has a resonance at 620.9 ppm ($^1J_{NW}$ = 68 Hz), which is nearly identical to that of $\{[Cp^*Me_3W]_2(\mu\text{-}N)\}PF_6$ (**13b**) at 634.9 ppm ($^1J_{NW}$ = 63 Hz), implying similar delocalized M=N=M structures. The tantalum methyl groups are equivalent in the proton NMR spectrum down to –80 °C, consistent with the proposed location of the triflate ligand trans to the nitride. The infrared spectrum of **14** has two vibrations at 1020 and 983 cm^{-1}, which upon ^{15}N substitution shift to 1012 and 964 cm^{-1}, respectively. The presence of strong triflate vibrations (at ~990 cm^{-1}) hinders assignment of these vibrations. As in the case of $[Cp^*Me_3W]_2(\mu\text{-}N)$ (**13a**), ν(MNM') for **14** cannot be assigned with certainty. The poor solubility of **15** has prevented the acquisition of an ^{15}N NMR spectrum in order to verify the W–N bonding mode. The structure of **15** is believed to be a fluxional square pyramid (cf. $(\eta^5\text{-}C_5H_5)TaMe_3Cl$[50]). Formation of a Ta–N π bond makes pseudorotation a higher energy process (there are two tantalum methyl resonances in the NMR spectrum of the amide $Cp^*TaMe_3(NMe_2)$[51]), which leads us to propose the localized, asymmetric "metalloimide" structure, W≡N—Ta. However, the fact that the tantalum methyl groups do not become inequivalent in the proton NMR spectrum upon cooling a sample to –80 °C does not permit us to rule out a trigonal-bipyramidal geometry at tantalum with the Cp* trans to the nitride ligand. A strong WNTa vibration in the infrared

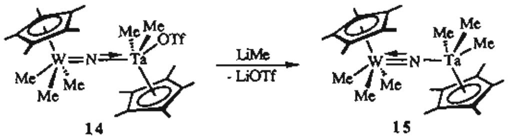

(13)

---

(41) Klein, C.; Tsay, Y.-H. *Angew. Chem., Int. Ed. Engl.* **1973**, *12*, 998.
(42) Jonas, K.; Brauer, D. J.; Kruger, C.; Roberts, P. J.; Tsay, Y.-H. *J. Am. Chem. Soc.* **1976**, *98*, 74 and references therein.
(43) Doherty, N. M.; Critchlow, S. C. *J. Am. Chem. Soc.* **1987**, *109*, 7906.
(44) Critchlow, S. C.; Lerchen, M. E.; Smith, R. C.; Doherty, N. M. *J. Am. Chem. Soc.* **1988**, *110*, 8071.
(45) Dehnicke, K.; Strahle, J. *Angew. Chem., Int. Ed. Engl.* **1981**, *20*, 413.
(46) Horner, M.; Frank, K.-P.; Strahle, J. *Z. Naturforsch.* **1986**, *41B*, 423.
(47) Frank, K.-P.; Strahle, J.; Weidlein, J. *Z. Naturforsch.* **1980**, *35B*, 300.
(48) Noble, M. E.; Folting, K.; Huffman, J. C.; Wentworth, R. A. D. *Inorg. Chem.* **1982**, *21*, 3772.
(49) Nugent, W. A.; Mayer, J. M. *Metal-Ligand Multiple Bonds*; Wiley: New York, 1988.
(50) Schrock, R. R.; Sharp, P. R. *J. Am. Chem. Soc.* **1978**, *100*, 2389.
(51) Mayer, J. M.; Curtis, C. J.; Bercaw, J. E. *J. Am. Chem. Soc.* **1983**, *105*, 2651.

spectrum of **15** shifts 31 cm^{-1} (from 1014 to 983 cm^{-1}) upon ^{15}N labeling, as expected.

Conclusions

The hydrazido(2−) ligand in $Cp^*Me_3W{=}NNH_2$ (**1**) reacts with a number of electrophilic main-group and transition-metal alkyl complexes to generate new bimetallic hydrazido(3− and 4−) complexes. The structures of the various lithium- and magnesium-substituted hydrazido(2−) derivatives appear to have close counterparts in the literature of organometallic complexes in which the metal is in a lower oxidation state than observed here. $[Cp^*Me_3W{=}NNH]_2[\mu\text{-}Mg(S)_n]$ has been used to prepare a number of bimetallic W–Zr and W–Ta hydrazido(3− and 4−) complexes. Nucleophilic displacement reactions using the lithiated imido complex $[Cp^*Me_3W{=}NLi]_x$ have yielded a number of homo- and heterobimetallic bridging-nitride complexes.

Many of the compounds isolated and examined herein support earlier proposals for the intermediacy of metalated imides and hydrazido species in the activation of dinitrogen using electropositive metals such as lithium and magnesium.[2] However, the potential of the metalated (M = Li, Mg, Ta, Zr) derivatives of **1** to act as intermediates in the reduction of dinitrogen to ammonia is limited by their facile hydrolysis back to the hydrazido(2−) complex **1**. In retrospect, this is not surprising in view of the ionic nature of the MN bonds, the oxophilicity of M, the lack of any significant amount of MN π bonding (in the Li and Mg compounds), and the presence of a strong tungsten–imido triple bond. Since **1** is now known to be reduced in the presence of protons to give nearly 2 equiv (1.80 equiv, 90% conversion) of ammonia,[52] we can conclude that electropositive metals bound to one end of N_2 (at least if a d^0 tungsten is bound to the other end) do not aid in further activation and subsequently reduction of dinitrogen. Other complexes that are easily hydrolyzed to form **1** also give high yields of ammonia upon bulk reduction, e.g. $Cp^*Me_3W{=}N{-}N{=}MoCp^*Me_3$ (1.75 equiv, 88%)[8] and $Cp^*MeW{=}N{-}N{=}TaCp^*Me_2$ (1.75 equiv, 88%). Bulk reduction of $Cp^*Me_3W{=}N{-}N{=}WCp^*Me_3$, which does not hydrolyze readily to form **1**, yields much less ammonia (0.84 equiv, 42%).[7]

Although symmetric bridging nitrides potentially could be reduced and protonated etc. to yield ammonia, the final stages of dinitrogen reduction probably would be more efficient if only monometallic species were involved. There is now good evidence that ammonia can be generated efficiently at a single metal center in Cp^*Me_3M systems of the general type discussed here and that the N–N bond is split in an η^2-hydrazine adduct.[52] Multimetallic activation of dinitrogen may still be most effective in situations where metal–nitrogen π bonding at one end of the dinitrogen is relatively insignificant.

Experimental Section

General Procedures. Solvents were dried and degassed prior to use by distillation from sodium (toluene), sodium/benzophenone (ether, tetrahydrofuran, pentane—using tetraglyme to solvate the sodium), or calcium hydride (dichloromethane). All syntheses were carried out either under a nitrogen atmosphere in a Vacuum Atmospheres drybox, under argon with Schlenk techniques, or on a high-vacuum line ($<10^{-4}$ Torr).

NMR operating frequencies and reference standards are as follows: ^1H (300.1 MHz, $SiMe_4$ = 0 ppm), ^{13}C (75.0 MHz, $SiMe_4$ = 0 ppm), ^6Li (44.1 MHz, 1.0 M $LiCl/D_2O$ = 0 ppm), ^7Li (116.6 MHz, 1.0 M $LiCl/D_2O$ = 0 ppm), ^{15}N (30.4 MHz, NH_2Ph = 56.5 ppm), ^{19}F (282.2 MHz, $CFCl_3$ = 0 ppm). Proton and carbon NMR data were referenced using resonances for the partially deuterated NMR solvent. Other nuclei were referenced externally in the same solvent unless otherwise noted. Chemical shifts are in ppm, and coupling constants and line widths are in hertz. All spectra were acquired at room temperature unless otherwise noted. ^{15}N NMR data can be found in Table I. Deuterated solvents were dried by passage through alumina and storage over 4-Å molecular sieves. ESR spectra were collected on a Bruker ESP 300 spectrometer in 3-mm quartz tubes at room temperature unless otherwise noted; the line width ($\Delta\nu_{1/2}$) is in parentheses and is reported in gauss in the solvent indicated.

Infrared spectra were acquired on a Mattson Cygnus 100 FT-IR spectrometer; absorptions are reported in units of cm^{-1}. All spectra were acquired on Nujol mulls between KBr plates, unless otherwise noted. Solution spectra were collected using airtight cells with KBr windows in the solvent indicated. UV–visible measurements were obtained using a Hewlett-Packard 8452A photodiode array spectrophotometer in airtight quartz cuvettes in the solvent indicated. Absorptions (λ) are recorded in units of nm, and molar absorptivities (ϵ) are given in parentheses. Microanalyses (C, H, N) were performed either by Schwarzkopf Laboratories (Woodside, NY) or in our own laboratory using a Perkin-Elmer PE2400 microanalyzer.

Cyclic voltammetric measurements were performed with a Princeton Applied Research (PAR) Model 175 universal programmer, a PAR Model 173 potentiostat, a Model 179 digital coulometer, and a PAR Model RE0089 X-Y recorder. Measurements were made in the three-electron configuration with a platinum auxiliary electrode, a Ag/Ag^+ reference electrode, and a 25-μm platinum wire working electrode (sealed in a soft-glass pipette and contacted with mercury). Dichloromethane was used as solvent, and tetraethylammonium tetrafluoroborate was used as electrolyte. A small amount of ferrocene was added at the end of each experiment as a reference.

The following were prepared as reported in the literature: $MgNp_2(TMEDA)$,[53] Cp^*TaMe_3Cl,[54] Cp^*TaMe_4,[20] Cp_2ZrMe_2,[55] $Cp_2Zr(CH_2Ph)_2$,[56] $[Cp^*WMe_4]PF_6$,[57] $Cp^*Me_3W{=}NNH_2$,[12] $[Cp^*Me_3W]_2(\mu\text{-}N_2)$,[7] and $[Cp^*Me_3W{=}NLi]_x$.[9] $[^{15}N_2H_6]SO_4$ was purchased from MSD Isotopes (Montreal, Canada) and deprotonated using liquid ammonia, as previously reported.[10]

Preparation of Compounds. $[Cp^*Me_3W{=}NNHLi]_x$ (2). (a) The addition of *n*-butyllithium (0.24 mmol, 1.02 equiv) in 2 mL of ether to a solution of $Cp^*Me_3W{=}NNH_2$ (0.092 g, 0.23 mmol) in 5 mL of ether at −40 °C resulted in the formation of a yellow-orange solution. After 15 min, insoluble $[Cp^*Me_3W{=}NNLi_2]_x$ (0.22 g, 0.05 mmol, 22%) was filtered off and the solvent was removed from the filtrate in vacuo. The residue was extracted with ether; crystallization from a minimum of ether/pentane at −40 °C yielded yellow-brown, crystalline $[Cp^*Me_3W{=}NNHLi]_x$ (0.049 g, 0.12 mmol, 53%): ^1H NMR (THF-d_8) δ 6.10 (br, 1 H, NH), 1.61 (s, 15 H, Cp*), −0.29 (s, 6 H, WMe_{cis}), −0.68 (s, 3 H, WMe_{trans}); ^{13}C NMR (THF-d_8) δ 102.58 (Cp*), 23.08 ($^1J_{CW}$ = 79, WMe_{trans}), 16.11 ($^1J_{CW}$ = 59, 2 WMe_{cis}), 9.63 (Cp*); IR (Nujol) 1263 (vs), 1170 (w), 1029 (m), 839 (m), 607 (m), 470 cm^{-1} (w).

(b) A solution of methanol (0.010 g, 0.31 mmol, 1.04 equiv) in 2 mL of ether was added to a solution of $[Cp^*Me_3W{=}NNLi_2]_x$ (0.12 g, 0.30 mmol) in 5 mL of ether and 1 mL of tetrahydrofuran. The solution changed from deep orange to green-yellow in color; after 5 min, LiOMe was filtered off and the solvent was removed in vacuo. Extraction with ether and recrystallization of the greenish white residue from ether/pentane at −40 °C yielded pale yellow, crystalline $[Cp^*Me_3W{=}NNHLi]_x$ (0.10 g, 0.25 mmol, 83%).

$[Cp^*Me_3W{=}^{15}N^{15}NHLi]_x$ was prepared similarly using $[Cp^*Me_3W{=}^{15}N^{15}NLi_2]_x$: ^1H NMR (THF-d_8) δ 6.00 (dd, $^1J_{NH}$ = 54, $^2J_{NH}$ = 5.8, NH).

$[Cp^*Me_3W{=}NNLi_2]_x$ (3). *n*-Butyllithium (0.87 mmol, 2.12 equiv) was added to a solution of $Cp^*Me_3W{=}NNH_2$ (0.16 g, 0.41 mmol) in 3 mL of ether at −20 °C. Gas evolution was accompanied by a change in color from pale yellow to red-orange. After 30 min, orange $[Cp^*Me_3W{=}NNLi_2]_x$ (0.16 g, mmol, 95%) was filtered off and rinsed with ether. Allowing the reaction to stand undisturbed overnight yielded orange-red crystals: ^1H NMR (THF-d_8, −80 °C) δ 1.41 (s, 15 H, Cp*), −0.98 (s, 6 H, WMe_{cis}), −1.01 (s, 3 H, WMe_{trans}); ^{13}C NMR (THF-d_8, −60 °C) δ 94.93 (Cp*), 10.57 (WMe_{trans}), 9.47 (Cp*), 3.12 (2 WMe_{cis}); ^1H NMR (THF-d_8, 20 °C) δ 1.52 (s, 15 H, Cp*), −0.70 (s, 6 H, WMe), −0.78 (s, 3 H, WMe); ^{13}C NMR (THF-d_8, 20 °C) δ 100.00 (Cp*), 10.34 (WMe_{trans}), 9.62 (Cp*), 6.96 ($^1J_{CW}$ = 59, 2 WMe_{cis}); IR (Nujol) 1430 (s), 1060 (m), 1024 (m), 631 cm^{-1} (m).

$[Cp^*Me_3W{=}^{15}N^{15}NLi_2]_x$ was prepared similarly using $Cp^*Me_3W{=}^{15}N^{15}NH_2$.

$[Cp^*Me_3W{=}NNH(MgCl)]_x$ (5). Neopentylmagnesium chloride (1.07 mmol, 1.10 equiv) was added to a solution of $Cp^*Me_3W{=}NNH_2$ (0.38 g, 0.97 mmol) in 5 mL of ether at −40 °C. After 30 min, yellow $[Cp^*Me_3W{=}NNH(MgCl)]_x$ (0.37 g, 0.81 mmol, 83%) was filtered off and rinsed with ether: ^1H NMR (C_6D_6) δ 5.56 (br, 1 H, NH), 1.78 (s,

---

(52) Schrock, R. R.; Glassman, T. E.; Vale, M. G. *J. Am. Chem. Soc.* **1991**, *113*, 725.

(53) Andersen, R. A.; Wilkinson, G. *J. Chem. Soc., Dalton Trans.* **1977**, 809.

(54) Sanner, R. D.; Carter, S. T.; Bruton, W. J., Jr. *J. Organomet. Chem.* **1982**, *240*, 157.

(55) Samuel, E.; Rausch, M. D. *J. Am. Chem. Soc.* **1973**, *95*, 6263.

(56) Fachinetti, G.; Fochi, G.; Floriani, C. *J. Chem. Soc., Dalton Trans.* **1977**, 1946.

(57) Liu, A. H.; Murray, R. C.; Dewan, J. C.; Santarsiero, B. D.; Schrock, R. R. *J. Am. Chem. Soc.* **1987**, *109*, 4282.

15 H, Cp*), 0.49 (s, 6 H, WMe$_{cis}$), 0.21 (s, 3 H, WMe$_{trans}$); IR (Nujol) 3221 cm^{-1} (w, NH).

Cp*Me$_3$W=NNH(SiMe$_3$). Excess trimethylchlorosilane (0.12 g, 1.06 mmol, 8.47 equiv) was added to a solution of [Cp*Me$_3$W=NNH]$_2$(μ-Mg(TMEDA)] (0.12 g, 0.12 mmol) in 5 mL of tetrahydrofuran. After 10 min, the solvent was removed in vacuo and the product was extracted twice with pentane in order to separate the pentane-soluble product from the magnesium salts. Beige crystalline Cp*Me$_3$W=NNH(SiMe$_3$) (0.11 g, 0.24 mmol, 95%) was isolated from the extract upon removal of pentane in vacuo. Recrystallization from a minimum of pentane at −40 °C yielded analytically pure yellow-brown crystals: ^{1}H NMR (C$_6$D$_6$) δ 5.12 (br, 1 H, NH), 1.61 (s, 15 H, Cp*), 0.71 (s, 6 H, WMe$_{cis}$), 0.39 (s, 3 H, WMe$_{trans}$), 0.05 (s, $^2J_{HSi}$ = 6.8, 9 H, SiMe$_3$); ^{13}C NMR (C$_6$D$_6$) δ 107.55 (Cp*), 29.32 ($^1J_{CW}$ = 74, WMe$_{trans}$), 20.80 ($^1J_{CW}$ = 56, 2 WMe$_{cis}$), 10.29 (Cp*), −0.13 ($^1J_{CSi}$ = 57, SiMe$_3$); IR (Nujol) 3290 (m, NH), 1351 (s), 1250 (s, SiMe$_3$), 1030 (m, CH$_3$), 860 (s, SiMe$_3$), 845 (s, SiMe$_3$), 752 (s), 601 (w), 497 cm^{-1} (w). Anal. Calcd for C$_{16}$H$_{34}$N$_2$SiW: C, 41.20; H, 7.35; N, 6.01. Found: C, 41.28, H, 7.71; N, 6.23.

Cp*Me$_3$W=^{15}N^{15}NH(SiMe$_3$) was prepared in a similar fashion using [Cp*Me$_3$W=^{15}N^{15}NHLi]$_x$: ^{1}H NMR (C$_6$D$_6$) δ 5.12 (dd, $^1J_{NH}$ = 82, $^2J_{NH}$ = 0.9, NH).

Cp*Me$_3$W=NNH(SiMe$_3$) also can be prepared by treating either [Cp*Me$_3$W=NNHLi]$_x$ or [Cp*Me$_3$W=NNH]$_2$[μ-Mg(TMEDA)] with excess trimethylchlorosilane.

Cp*Me$_3$W=NN(SiMe$_3$)$_2$. Excess trimethylchlorosilane (500 μL, 3.93 mmol, 5.87 equiv) was added to a solution of [Cp*Me$_3$W=NNLi$_2$]$_x$ (0.27 g, 0.67 mmol) in 10 mL of tetrahydrofuran at −40 °C. After 15 min, the solvent was removed in vacuo and the resulting light yellow residue was extracted with pentane. Pale yellow, crystalline Cp*Me$_3$W=NN(SiMe$_3$)$_2$ (0.27 g, 0.50 mmol, 75%) was obtained by removing the pentane in vacuo. Recrystallization from a minimum of pentane at −40 °C yielded analytically pure yellow needles: ^{1}H NMR (C$_6$D$_6$) δ 1.61 (s, 15 H, Cp*), 0.71 (s, 6 H, WMe$_{cis}$), 0.39 (s, 3 H, WMe$_{trans}$), 0.05 (s, $^2J_{HSi}$ = 6.8, 18 H, SiMe$_3$); ^{13}C NMR (C$_6$D$_6$) δ 108.07 (Cp*), 28.25 ($^1J_{CW}$ = 78, WMe$_{trans}$), 21.19 ($^1J_{CW}$ = 57, 2 WMe$_{cis}$), 10.56 (Cp*), 2.16 ($^1J_{CSi}$ = 57, SiMe$_3$); IR (Nujol) 1286 (s, SiMe$_3$), 1250 (s, SiMe$_3$), 1024 (w, CH$_3$), 936 (s, SiMe$_3$), 860 (s, SiMe$_3$), 844 (s, SiMe$_3$), 824 (sh), 780 (m), 758 (m), 676 (m), 620 (w), 559 (w), 521 (w), 495 (w), 464 (w), 451 cm^{-1} (w). Anal. Calcd for C$_{19}$H$_{42}$N$_2$Si$_2$W: C, 42.37; H, 7.86; N, 5.20. Found: C, 42.45; H, 8.06; N, 4.98.

Cp*Me$_3$W=^{15}N^{15}N(SiMe$_3$)$_2$ was prepared in a similar fashion using [Cp*Me$_3$W=^{15}N^{15}NLi$_2$]$_x$.

Cp*Me$_3$W=NN(SiMe$_3$)$_2$ also can be prepared by generating [Cp*Me$_3$W=NNLi$_2$]$_x$ in situ or by using [Cp*Me$_3$W=NN]$_2$[μ-Mg-(TMEDA)]$_2$.

[Cp*Me$_3$W=NNH]$_2$[μ-Mg(TMEDA)] (6-TMEDA). A solution of MgNp$_2$(TMEDA) (0.10 g, 0.35 mmol) in 5 mL of ether was added to a solution of Cp*Me$_3$W=NNH$_2$ (0.27 g, 0.69 mmol) in 10 mL of ether at room temperature. After 30 min, yellow [Cp*Me$_3$W=NNH]$_2$[μ-Mg(TMEDA)] (0.30 g, 0.32 mmol, 91%) was filtered off and rinsed with ether: ^{1}H NMR (C$_6$D$_6$) δ 5.50 (br, 1 H, NH), 1.95 (s, 6 H, NCH$_3$), 1.62 (s, 2 H, NCH$_2$), 1.74 (s, 15 H, Cp*), 0.48 (s, 6 H, WMe$_{cis}$), 0.25 (s, 3 H, WMe$_{trans}$); ^{13}C NMR (C$_6$D$_6$) δ 105.1 (Cp*), 55.61 (TMEDA, CH$_2$), 45.82 (TMEDA, Me), 26.29 (WMe$_{trans}$), 18.74 (2 WMe$_{cis}$), 9.82 (Cp*); IR (Nujol) 3196 cm^{-1} (m, NH).

[Cp*WMe$_3$(NNH)]$_2$[μ-Mg(THF)$_n$] (6-(THF)$_n$). [Cp*WMe$_3$-(NNH)]$_2$[μ-Mg(TMEDA)] (0.30 g, 0.33 mmol) was dissolved in 3 mL of tetrahydrofuran. Yellow, crystalline [Cp*Me$_3$W=NNH)]$_2$[μ-Mg-(THF)$_4$] was formed upon addition of excess pentane and storage at −40 °C. Upon rinsing with pentane or exposure to vacuum, 2 equiv of THF was lost and yellow [Cp*Me$_3$W=NNH)]$_2$[μ-Mg(THF)$_2$] (0.21 g, 0.22 mmol, 67%) was formed: ^{1}H NMR (THF-d_8) δ 5.34 (br, 1 H, NH), 3.62 (m, 8 H, THF), 1.78 (m, 8 H, THF), 1.64 (s, 30 H, Cp*), −0.15 (s, 12 H, WMe$_{cis}$), −0.55 (s, 6 H, WMe$_{trans}$); ^{13}C NMR (THF-d_8) δ 104.10 (Cp*), 68.21 (THF), 26.42 (THF), 17.1 (WMe$_{cis}$ and WMe$_{trans}$), 9.62 (Cp*).

[Cp*Me$_3$W=^{15}N^{15}NH]$_2$[μ-Mg(THF)$_2$] was prepared similar from [Cp*Me$_3$W=^{15}N^{15}NH]$_2$[μ-Mg(TMEDA)]: ^{1}H NMR (THF-d_8) δ 5.40 (d, $^1J_{NH}$ = 59, NH).

[Cp*Me$_3$W=NNH]$_2$[μ-Mg(DME)] (6-DME). The procedure is the same as for the preparation of the THF adduct using dimethoxyethane: ^{1}H NMR (C$_6$D$_6$) δ 5.57 (br, 2 H, NH), 3.22 (br, 10 H, DME), 1.77 (s, 30 H, Cp*), 0.44 (s, 12 H, WMe$_{cis}$), 0.23 (s, 6 H, WMe$_{trans}$).

[Cp*Me$_3$W=NNH)]$_2$[μ-Mg(py)$_4$] (6-(py)$_4$). The procedure is the same as for the preparation of the THF adduct using pyridine: ^{1}H NMR (C$_6$D$_6$) δ 8.65 (d, 8 H, py H$_\alpha$), 6.91 (tr, 4 H, py H$_\gamma$), 6.72 (tr, 8 H, py H$_\beta$), 5.88 (br, 2 H, NH), 1.75 (s, 30 H, Cp*), 0.44 (s, 12 H, WMe$_{cis}$), 0.23 (s, 6 H, WMe$_{trans}$).

Cp*Me$_3$W=NNH[MgNp(TMEDA)] (7). (a) A solution of Cp*Me$_3$W=NNH$_2$ (0.091 g, 0.23 mmol) in 2 mL of ether was added quickly to a solution of MgNp$_2$(TMEDA) (0.065 g, 0.23 mmol, 1.00 equiv) in 2 mL of ether, and the mixture was then stored at −40 °C for 1.5 h. The orange-red solution was layered with cold pentane and pale yellow, crystalline Cp*Me$_3$W=NNH-[MgNp(TMEDA)] (0.032 g, 0.053 mmol, 23%) was isolated and rinsed with pentane: ^{1}H NMR (THF-d_8) δ 5.55 (br, 1 H, NH), 1.66 (s, 15 H, Cp*), 0.97 (s, 9 H, CH$_2$C*Me*$_3$), −0.11 (s, 6 H, WMe$_{cis}$), −0.37 (s, 3 H, WMe$_{trans}$), −0.39 (s, 2 H, C*H*$_2$CMe$_3$). Free TMEDA was observed, having been displaced by tetrahydrofuran.

(b) A solution of [Cp*Me$_3$W=NNH]$_2$[μ-Mg(TMEDA)] in ether was added to a solution of MgNp$_2$(TMEDA) in ether, and the mixture was stored at −40 °C for 2 h. Yellow crystalline Cp*Me$_3$W=NNH-[MgNp(TMEDA)] was filtered off and rinsed with cold ether.

[Cp*Me$_3$W=NN]$_2$[μ-Mg(TMEDA)]$_2$ (8). (a) A mixture of MgNp$_2$(TMEDA) (0.084 g, 0.32 mmol) and Cp*Me$_3$W=NNH$_2$ (0.12 g, 0.31 mmol) was dissolved in a minimum amount (5 mL) of toluene. The orange solution turned green after 30 min. After 16 h, feathery, red needles of [Cp*Me$_3$W=NN]$_2$[μ-Mg(TMEDA)]$_2$ (0.091 g, 0.17 mmol, 55%) were filtered off and rinsed with ether: ^{1}H NMR (THF-d_8) δ 2.34 (s, 8 H, NC*H*$_2$), 2.18 (s, 12 H, NC*H*$_3$), 1.55 (s, 30 H, Cp*), −0.56 (s, 12 H, WMe$_{cis}$), −0.86 (s, 6 H, WMe$_{trans}$); ^{13}C NMR (THF-d_8) δ 101.47 (Cp*), 58.46 (NMe), 46.48 (NCH$_2$), 18.36 (WMe$_{trans}$), 14.40 (WMe$_{cis}$), 9.83 (Cp*).

[Cp*Me$_3$W=^{15}N^{15}N]$_2$[Mg(TMEDA)]$_2$ was prepared similarly from Cp*Me$_3$W=^{15}N^{15}NH$_2$.

(b) Warming a solution of Cp*Me$_3$W=NNH[MgNp(TMEDA)] in ether from −40 °C to room temperature yielded [Cp*Me$_3$W=NN]$_2$-[Mg(TMEDA)]$_2$ according to the proton NMR spectrum.

Cp*Me$_3$W=N—N=TaCp*Me$_2$ (9). (a) A solution of Cp*TaMe$_3$Cl (0.11 g, 0.26 mmol) in 5 mL of ether was added to a slurry of [Cp*Me$_3$W=NNH]$_2$[Mg(DME)] (0.12 g, 0.14 mmol) in 5 mL of ether at −40 °C. The color immediately changed from yellow to orange-red. After 20 min, pentane was added and white MgCl$_2$ was filtered off. The solvent was removed from the filtrate in vacuo to yield red-orange Cp*Me$_3$W=N—N=TaCp*Me$_2$ (0.095 g, 0.13 mmol, 49%): ^{1}H NMR (C$_6$D$_6$) δ 1.75 (s, 15 H, TaCp*), 1.72 (s, 15 H, WCp*), 1.04 (s, 6 H, WMe$_{cis}$), 0.68 (s, 3 H, WMe$_{trans}$), 0.19 (s, 6 H, TaMe); ^{13}C NMR (C$_6$D$_6$) δ 116.66 (TaCp*), 108.56 (WCp*), 49.05 (TaMe), 30.96 ($^1J_{CW}$ = 73, WMe$_{trans}$), 22.03 ($^1J_{CW}$ = 56, WMe$_{cis}$), 10.31 (Cp*), 9.61 (Cp*); IR (C$_6$H$_6$) 890 cm^{-1} (s, WN, TaN); UV–vis (pentane) 216, 239, 314. Anal. Calcd for C$_{25}$H$_{45}$N$_2$TaW: C, 40.66; H, 6.14; N, 3.79. Found: C, 40.74; H, 6.25; N, 3.57.

Cp*Me$_3$W=^{15}N—^{15}N=TaCp*Me$_2$ was prepared similarly from [Cp*Me$_3$W=^{15}N^{15}NH]$_2$[Mg(TMEDA)]: IR (Nujol) 863 cm^{-1} (s, WNNTa).

(b) A solution of Cp*TaMe$_4$ (0.090 g, 0.24 mmol) in 5 mL of ether was added to a solution of Cp*Me$_3$W=NNH$_2$ (0.094 g, 0.24 mmol) in 10 mL of ether. After 7 h, the reaction was complete according to the proton NMR spectrum. Cp*Me$_3$W=N—N=TaCp*Me$_2$ (0.064 g, 0.086 mmol, 36%) was isolated from a minimum quantity of tetrahydrofuran by adding ether and storing the solution at −40 °C.

Hydrolysis of Cp*Me$_3$W=N—N=TaCp*Me$_2$. Addition of excess water to Cp*Me$_3$W=N—N=TaCp*Me$_2$ dissolved in ether cleanly yielded Cp*WMe$_3$(NNH$_2$) and insoluble white [Cp*TaMe$_2$O]$_x$, after stirring the mixture at room temperature for 30 min.

Protonolysis of Cp*Me$_3$W=N—N=TaCp*Me$_2$. Addition of 2 equiv of triflic acid to a solution of Cp*Me$_3$W=N—N=TaCp*Me$_2$ in ether yielded primarily [Cp*WMe$_3$(η^2-NHNH$_2$)]OTf[10] and Cp*TaMe$_2$(OTf)$_2$.

Cp*Me$_3$W=NNH(ZrCp$_2$Me) (10a). A solution of Cp*Me$_3$W=NNH$_2$ (0.30 g, 0.76 mmol) in 3 mL of ether was added to a solution of Cp$_2$ZrMe$_2$ (0.19 g, 0.76 mmol) in 15 mL of ether at room temperature; the solution slowly became bright orange. After 16 h, the solvent was removed in vacuo and the residue was recrystallized from tetrahydrofuran/pentane at −40 °C to yield analytically pure orange-yellow, crystalline Cp*Me$_3$W=NNH(ZrCp$_2$Me) (0.31 g, 0.50 mmol, 66%): ^{1}H NMR (C$_6$D$_6$) δ 8.03 (s, 1 H, NH), 5.70 (s, 10 H, ZrCp), 1.61 (s, 15 H, WCp*), 0.85 (s, 6 H, WMe$_{cis}$), 0.57 (s, 3 H, WMe$_{trans}$), 0.27 (s, 3 H, ZrMe); ^{13}C NMR (C$_6$D$_6$) δ 110.40 (ZrCp$_2$), 107.29 (WCp*), 28.03 (WMe$_{trans}$), $^1J_{CW}$ = 74), 21.90 (ZrMe), 20.79 (WMe$_{cis}$, $^1J_{CW}$ = 56); IR (Nujol) 3244 (vw, NH?), 1290 (s), 1251 (sh), 1177 (m), 1032 (m), 1027 (m), 1012 (m), 799 (s, Cp), 683 (m), 647 (m), 519 (w), 452 cm^{-1} (w); UV–vis (THF) 228, 257 sh, 380. Anal. Calcd for C$_{24}$H$_{38}$N$_2$WZr: C, 45.78; H, 6.08; N, 4.45. Found: C, 45.49; H, 6.27; N, 4.48.

Cp*Me$_3$W=NNH(ZrCp$_2$Bz) (10b). This compound was prepared from Cp$_2$ZrBz$_2$ in a manner similar to that used to prepare Cp*Me$_3$=NNH(ZrCp$_2$Me): ^{1}H NMR (C$_6$D$_6$) δ 8.11 (s, 1 H, NH), 7.30 (tr, 2 H, H$_m$), 7.09 (d, 2 H, H$_o$), 6.96 (tr, 1 H, H$_p$), 5.57 (s, 10 H, ZrCp), 2.23 (s, 2 H, ZrCH$_2$), 1.67 (s, 15 H, WCp*), 0.92 (s, 6 H, WMe$_{cis}$), 0.58 (s, 3 H, WMe$_{trans}$); ^{13}C NMR (C$_6$D$_6$) δ 155.27 (C$_{ipso}$), 128.06 (C$_{o/mol}$), 127.76 (C$_{o/m}$), 120.38 (C$_p$), 111.96 (ZrCp), 108.22 (Cp*), 51.22

(C*H*$_2$Ph), 28.19 ($^1J_{CW}$ = 74, WMe$_{trans}$), 20.78 ($^1J_{CW}$ = 56, WMe$_{cis}$), 10.18 (Cp*).

[Cp*Me$_3$W=NNH]$_2$ZrCp$_2$ (11). A mixture of Cp*Me$_3$W=NNH$_2$ (0.10 g, 0.26 mmol) and ZrCp$_2$Me$_2$ (0.032 g, 0.13 mmol, 0.50 equiv) was dissolved in a minimum of ether (3 mL) at room temperature. The solution slowly changed from beige to orange, and after 46 h, orange-red [Cp*Me$_3$W=NNH]$_2$ZrCp$_2$ (0.045 g, 0.045 mmol, 35%) had precipitated and was isolated by filtration and washed with −40 °C ether. Recrystallization from toluene/pentane at −40 °C yielded orange plates: ^{1}H NMR (C$_6$D$_6$) δ 7.81 (s, 2 H, NH), 5.76 (s, 10 H, ZrCp), 1.77 (s, 30 H, WCp*), 0.82 (s, 12 H, WMe$_{cis}$), 0.54 (s, 6 H, WMe$_{trans}$); ^{13}C NMR (THF-d_8) δ 107.77 (Cp*), 112.61 (Cp), 27.69 (WMe$_{trans}$), 20.33 (2 WMe$_{cis}$), 10.14 (Cp*).

[Cp*Me$_3$W=^{15}N^{15}NH]$_2$ZrCp$_2$ was prepared similarly from Cp*Me$_3$W^{15}N^{15}NH$_2$: ^{1}H NMR (C$_6$D$_6$) δ 7.81 (dd, $^1J_{NH}$ = 71, $^2J_{NH}$ = 3).

Proton NMR Spectrum of Cp*$_3$W$_3$Zr$_2$Cp$_4$Me$_7$N$_x$. ^{1}H NMR (CD$_2$Cl$_2$): δ 6.09 (s, 5 H, ZrCp), 5.99 (s, 5 H, ZrCp), 5.83 (s, 5 H, ZrCp), 5.79 (s, 5 H, ZrCp), 2.14 (s, 15 H, WCp*), 1.92 (s, 15 H, WCp*), 1.89 (s, 15 H, WCp*), 0.85 (s, 3 H, Me), 0.78 (s, 3 H, Me), 0.60 (s, 3 H, Me), 0.48 (s, 3 H, Me), 0.47 (s, 3 H, Me), 0.18 (s, 3 H, Me), −0.25 (s, 3 H, Me).

Cp*Me$_3$W=N—N=WCp*Me$_2$(OTf). A solution of triflic acid (0.011 g, 0.073 mmol, 1.09 equiv) in 2 mL of ether was added to a solution of Cp*Me$_3$W=N—N=WCp*Me$_3$ (0.051 g, 0.067 mmol) in 5 mL of ether at −40 °C. After the mixture was stirred for 15 min, Cp*Me$_3$W=N—N=WCp*Me$_2$(OTf) (0.043 g, 0.048 mmol, 72%) precipitated as a beige powder and was filtered off and rinsed with cold ether. Recrystallization from dichloromethane/pentane yielded analytically pure copper-colored plates: ^{1}H NMR (CD$_2$Cl$_2$) δ 1.97 (s, 15 H, Cp*), 1.94 (s, 15 H, Cp*), 0.98 (s, 6 H, WMe$_{cis}$), 0.66 (s, 6 H, WMe$_{cis}$), 0.42 (s, 3 H, WMe$_{trans}$); ^{13}C NMR (THF-d_8) δ 114.83 (Cp*), 112.16 (Cp*), 41.79 (WMe$_{trans}$), 38.53 ($^1J_{CW}$ = 55, 2 WMe$_{cis}$), 30.55 ($^1J_{CW}$ = 55, 2 WMe$_{cis}$), 11.03 (Cp*), 10.86 (Cp*); ^{19}F NMR (CD$_2$Cl$_2$) δ −78.5 (OTf); IR (Nujol) 1328 (s), 1228 (s), 1197 (vs, OTf), 1176 (s), 1010 (s, OTf), 883 (s, WN), 617 (s, OTf), 497 (w), 485 (w), 1328 (s), 1228 (s), 1197 (vs, OTf), 1176 (s), 1010 (s, OTf), 883 (s, WN), 617 (s, OTf), 497 (w), 485 cm^{-1} (w); UV-vis (THF) 215, 262, 298, 346. Anal. Calcd for C$_{26}$H$_{45}$F$_3$N$_2$O$_3$SW$_2$: C, 35.07; H, 5.09; N, 3.15. Found: C, 35.06; H, 4.93; N, 3.10.

[Cp*Me$_3$W]$_2$(μ-N) (13a). (a) Cp*Me$_3$W(OTf) (0.41 g, 0.81 mmol, 1.00 equiv) in 5 mL of ether was added to [Cp*Me$_3$W=NLi]$_x$ (0.31 g, 0.81 mmol) in 15 mL of ether at room temperature. After 15 min, dark green, crystalline [Cp*Me$_3$W]$_2$(μ-N) (0.57 g, 0.76 mmol, 94%) was isolated by filtration and rinsed with ether in order to remove the LiOTf. Recrystallization from dichloromethane/ether gave analytically pure, green, hexagonal crystals: ESR (CH$_2$Cl$_2$) ⟨*g*⟩ = 1.916 (119 G); CV (CH$_2$Cl$_2$) E_{ox} = −0.697 V, E_{red} = −0.775 V vs $E_{1/2}$ for FeCp$_2^{+/0}$; IR (Nujol) 1026 (m, CH$_3$), 800 (m, WNW), 655 (w), 488 cm^{-1} (m); UV–vis (CH$_2$Cl$_2$) 232 (31 000), 292 (13 000), 344 (14 000), 418 (sh, 5700), 484 (sh, 2500), 606 (700). Anal. Calcd for C$_{26}$H$_{48}$NW$_2$: C, 42.07; H, 6.52; N, 1.89. Found: C, 42.41; H, 6.77; N, 2.02.

[Cp*Me$_3$W]$_2$(μ-^{15}N) was prepared similarly from [Cp*Me$_3$W=^{15}NLi)]$_x$: IR (Nujol) 1026 (m, CH$_3$), 789 (m, WNW), 652 (w), 488 cm^{-1} (m).

(b) Reduction of {[Cp*Me$_3$W]$_2$(μ-N)}PF$_6$ (0.058 g, 0.066 mmol) in tetrahydrofuran with 0.5% sodium/amalgam at −40 °C yields [Cp*Me$_3$W]$_2$(μ-N) quantitatively.

{[Cp*Me$_3$W]$_2$(μ-N)}PF$_6$ (13b). Solid [FeCp$_2$]PF$_6$ (0.041 g, 0.12 mmol) was added to a slurry of [Cp*Me$_3$W]$_2$(μ-N) (0.082 g, 0.11 mmol) in 10 mL of dichloromethane. The solution turned red, and after 15 min, the solvent was removed in vacuo and FeCp$_2$ was removed from the filtrate by extraction with ether, leaving deep red {[Cp*Me$_3$W]$_2$(μ-N)}PF$_6$ (0.075 g, 0.084 mmol, 77%) as a powder. Recrystallization from dichloromethane/ether at −40 °C yielded analytically pure, deep red crystals: ^{1}H NMR (CD$_2$Cl$_2$) δ 1.98 (s, 15 H, Cp*), 1.32 (s, 6 H, WMe$_{cis}$), 1.02 (s, 3 H, WMe$_{trans}$); ^{13}C NMR (CD$_2$Cl$_2$) δ 115.85 (Cp*), 57.23 ($^1J_{CW}$ = 47, WMe$_{trans}$), 51.95 ($^1J_{CW}$ = 52, WMe$_{cis}$), 11.08 (Cp*); ^{19}F NMR (CD$_2$Cl$_2$) δ −73.35 ($^1J_{FP}$ = 706, PF$_6$); IR (Nujol) 1169 (m), 1029 (m, PF$_6$, CH$_3$), 999 (s, WNW), 877 (m), 843 (s, PF$_6$), 714 (m), 558 (m, PF$_6$), 494 (m), 453 cm^{-1} (w); UV-vis (CH$_2$Cl$_2$) 232 (11 000), 262 (sh, 7400), 300 (6100), 366 (5300), 402 (sh, 4500), 558 (sh, 800). Anal. Calcd for C$_{26}$H$_{48}$F$_6$NPW$_2$: C, 35.19; H, 5.45; N, 1.58. Found: C, 34.86; H, 5.22; N, 1.42.

{[Cp*Me$_3$W]$_2$(μ-^{15}N)}PF$_6$ was prepared similarly using [Cp*Me$_3$W]$_2$(μ-^{15}N): IR (Nujol) 1169 (m), 1025 (m, PF$_6$, CH$_3$), 969 (s, W^{15}NW), 878 (m), 838 (s, PF$_6$), 713 (m), 558 (m, PF$_6$), 493 (m), 453 cm^{-1} (w).

TaCp*Me$_3$(OTf). A solution of triflic acid (0.028 g, 0.19 mmol, 0.99 equiv) in 2 mL of ether was added to a solution of Cp*TaMe$_4$ (0.071 g, 0.19 mmol) in 5 mL of ether at −40 °C. After 30 min, the solvent was removed in vacuo, yielding yellow Cp*TaMe$_3$(OTf) (0.094 g, 0.18 mmol, 98%): ^{1}H NMR (CD$_2$Cl$_2$) δ 2.10 (s, 15 H, Cp*), 0.69 (s, 9 H, Me); ^{13}C NMR (CD$_2$Cl$_2$) δ 122.25 (Cp*), 119.72 ($^1J_{CF}$ = 317, OTf), 76.25 (Me), 11.82 (Cp*); ^{19}F NMR (CD$_2$Cl$_2$) δ −78.2; IR (Nujol) 1351 (s), 1237 (s), 1194 (vs), 1158 (s), 989 (vs), 832 (w), 800 (w), 631 (s), 567 (m), 510 (m), 463 cm^{-1} (w).

TaCp*Me$_2$(OTf)$_2$. A solution of triflic acid (0.19 g, 1.26 mmol, 2.00 equiv) in 2 mL of ether was added to a solution of Cp*TaMe$_4$ (0.24 g, 0.63 mmol) in 10 mL of ether at room temperature. After evolution of gas ceased (ca. 30 min), the solvent was removed in vacuo, yielding yellow Cp*TaMe$_2$(OTf)$_2$. Recrystallization from a minimum of tetrahydrofuran/ether/pentane yielded analytically pure yellow crystals: ^{1}H NMR (CD$_2$Cl$_2$) δ 2.32 (s, 15 H, Cp*), 1.26 (s, 6 H, Me); ^{13}C NMR (CD$_2$Cl$_2$) δ 128.59 (Cp*), 82.28 (Me), 12.16 (Cp*); ^{19}F NMR (CD$_2$Cl$_2$) δ −77.2; IR (Nujol) 1366 (s), 1240 (s), 1191 (vs), 1164 (s), 1029 (w), 984 (vs), 944 (vs), 836 (w), 768 (w), 629 (s), 597 (m), 578 (w), 518 (m), 482 (m), 447 cm^{-1} (w). Anal. Calcd for C$_{14}$H$_{21}$F$_6$O$_6$S$_2$Ta: C, 26.01; H, 3.28. Found: C, 26.38; H, 3.48.

Cp*Me$_3$W(μ-N)TaCp*Me$_2$(OTf) (14). A slurry of Cp*TaMe$_2$(OTf)$_2$ (0.12 g, 0.18 mmol, 0.99 equiv) in 5 mL of ether was added to a slurry of [Cp*Me$_3$W=NLi]$_x$ (0.068 g, 0.18 mmol) in 10 mL of ether and 5 mL of tetrahydrofuran at −40 °C. After 15 min, the color of the solution while warming to room temperature, changed from yellow to orange. The solvent was removed in vacuo, and the residue was extracted with dichloromethane to remove insoluble LiOTf. The solvent was removed in vacuo from the filtrate, and crystallization from a minimum of ether/pentane at −40 °C yielded analytically pure red crystals of Cp*Me$_3$W(μ-N)TaCp*Me$_2$(OTf) (0.087 g, 0.10 mmol, 59%): ^{1}H NMR (CD$_2$Cl$_2$) δ 2.13 (s, 15 H, TaCp*), 1.90 (s, 15 H, WCp*), 1.06 (s, 6 H, WMe$_{cis}$), 0.55 (s, 6 H, TaMe), 0.33 (s, 3 H, WMe$_{trans}$); IR (Nujol) 1335 (s), 1232 (s), 1203 (vs, OTf), 1190 (sh), 1164 (m), 1020 (s), 981 (vs, WNTa), 832 (m), 622 (m, OTf), cm^{-1} 482 (w). Anal. Calcd for C$_{26}$H$_{45}$F$_3$NO$_3$STaW: C, 35.75; H, 5.19; N, 1.60. Found: C, 35.95; H, 5.13; N, 1.27.

Cp*Me$_3$W(μ-^{15}N)TaCp*Me$_2$(OTf) was prepared in a similar fashion using [Cp*Me$_3$W=^{15}NLi]$_x$: ^{15}N NMR (CD$_2$Cl$_2$) δ 620.9 ($^1J_{NW}$ = 68); IR (Nujol) 1335 (s), 1232 (s), 1204 (vs, OTf), 1190 (sh), 1164 (m), 1012 (s), 964 (vs, WNTa), 622 (s, OTf), 482 cm^{-1} (w).

Cp*Me$_3$W(μ-N)TaCp*Me$_3$ (15). (a) A solution of [Cp*Me$_3$W=NLi]$_x$ (0.030 g, 0.078 mmol) in 5 mL of ether was added to a solution of Cp*TaMe$_3$Cl (0.031 g, 0.078 mmol) in 2 mL of ether at room temperature. After 10 min, orange, crystalline Cp*Me$_3$W(μ-N)TaCp*Me$_3$ (0.051 g, 0.069 mmol, 89%) was filtered off and rinsed with ether. Recrystallization from dichloromethane/ether yielded analytically pure, orange crystals: ^{1}H NMR (CD$_2$Cl$_2$) δ 1.98 (s, 15 H, Cp*), 1.32 (s, 6 H, WMe$_{cis}$), 1.02 (s, 3 H, WMe$_{trans}$); IR (Nujol) 1172 (w), 1153 (m), 1129 (w), 1037 (Me), 1014 (vs, WNTa), 833 (m), 797 (w), 620 (vw), 490 (m), 482 cm^{-1} (m). Anal. Calcd for C$_{26}$H$_{48}$NTaW: C, 42.33; H, 6.54; N, 1.89. Found: C, 42.20; H, 6.93; N, 1.61.

(b) An excess of methyllithium was added to a solution of Cp*Me$_3$W(μ-N)TaCp*Me$_2$(OTf) in 5 mL of ether at room temperature. After 5 min, yellow-orange, crystalline Cp*Me$_3$W(μ-N)TaCp*Me$_3$ was collected by filtration and rinsed with ether.

Cp*WMe$_3$(μ-^{15}N)TaCp*Me$_3$ was prepared similarly using Cp*Me$_3$W(μ-^{15}N)TaCp*Me$_2$(OTf): IR (Nujol) 1172 (w), 1030 (m, Me), 998 (sh), 983 (vs, WNTa), 796 (w), 488 (w), 467 cm^{-1} (w).

Structure of [Cp*Me$_3$W=NNH]$_2$[μ-Mg(THF)$_4$] (6-(THF)$_4$). Crystallization of **6**-(THF)$_4$ from a mixture of tetrahydrofuran and pentane yielded yellow blocks. A crystal having the approximate dimensions of 0.250 × 0.200 × 0.320 mm was mounted on a glass fiber, and data were collected at −65 °C as described fully in the supplementary material. The structure could be solved, but not refined well enough to allow any discussion of bond lengths and angles.

Structure of [Cp*Me$_3$W]$_2$(μ-N) (13a). Crystallization of **13a** from a solution of dichloromethane/ether yielded green parallelepipeds. A crystal having the approximate dimensions of 0.220 × 0.180 × 0.320 mm was mounted on a glass fiber. Data were collected at −78 °C on an Enraf-Nonius CAD-4 diffractometer with graphite-monochromated Mo Kα radiation (λ = 0.71073 Å). A total of 3315 reflections were collected in the range 3.00° < 2θ < 55.00°, with 3117 being unique. No crystal decay was evident during data collection. An empirical absorption correction was applied, using the program DIFABS, which resulted in transmission factors ranging from 0.83 to 1.36. The structure was solved by the Patterson method. The non-hydrogen atoms were refined either anisotropically or isotropically. The methyl groups on the Cp* ligand could not be refined anisotropically. Hydrogen atoms were included in the structure factor calculation in idealized positions. The final cycle of

Table IV. Crystallographic Data for **6**-$(THF)_4$ and **13a**

chem formula	$[Cp^*Me_3W{=}NNH]_2[\mu\text{-}Mg(THF)_4]$[a]	$[Cp^*Me_3W]_2(\mu\text{-}N)$
a, Å	12.380 (6)	8.390 (4)
b, Å	15.252 (6)	20.341 (6)
c, Å	30.618 (8)	8.733 (4)
β, deg	97.91 (3)	117.83 (2)
V, Å^3	5726 (7)	1318 (2)
Z, molecules/cell	4	2
MW	1099.14	742.37
space group (No. 14)	$P2_1/n$	$P2_1/c$
λ, Å	0.710 73	0.710 73
ρ(calcd), g/cm^3	1.275	1.870
μ, cm^{-1}		89.21
R[b]	0.082	0.057
R_w[c]	0.132	0.063

[a] The structure of **6**-$(THF)_4$ could not be refined adequately, although the connectivity was established unequivocally. Full details are provided in the supplementary material. [b] $R = \sum||F_o| - |F_c||/\sum|F_o|$. [c] $R_w = [\sum w(|F_o| - |F_c|)^2/\sum wF_o^2]^{1/2}$.

full-matrix least-squares refinement was based on 2011 reflections ($I > 3.00\sigma(I)$) and 108 variables and used the TEXSAN crystallographic software package from the Molecular Structure Corp. The final refinement converged with final $R = 0.057$ and $R_w = 0.063$. The maximum and minimum peaks on the final Fourier difference map corresponded to 2.29 and −2.08 e/Å^3, respectively. Crystal data can be founde in Table IV.

Acknowledgment. R.R.S. thanks the National Institutes of Health for support through Grant GM 31978 and T.E.G. thanks the National Science Foundation for a graduate fellowship. We thank M. G. Vale for quantifying the bulk hydrolysis of **9** and determining the structure of **13a** and Dr. W. M. Davis of the MIT Chemistry Department X-ray Diffraction Facility for valuable assistance with the solution of **6**-$(THF)_4$. We also thank J. F. Payack, Jr., for the preparation and analysis of $Cp^*Me_3W{=}NN(SiMe_3)_2$.

Supplementary Material Available: A labeled ORTEP drawing of **13a**, tables of final positional and thermal parameters for **13a**, a description of the X-ray study of **6**-$(THF)_4$, and tables of final positional and thermal parameters for **6**-$(THF)_4$ (11 pages); listings of final observed and calculated structure factors for **13a** and **6**-$(THF)_4$ (34 pages). Ordering information is given on any current masthead page.

---

(58) Payack, J. F., Jr. S.M. Thesis, MIT, 1987.

Contribution from the School of Chemical Sciences, University of Illinois at Urbana-Champaign,
505 South Mathews Avenue, Urbana, Illinois 61801

Characterization of Silica-Supported Osmium Carbonyl Clusters by Magic-Angle-Spinning Carbon-13 NMR Spectroscopy

Thomas H. Walter, Greg R. Frauenhoff, John R. Shapley, and Eric Oldfield*

Received June 5, 1991

We report the carbon-13 magic-angle-spinning nuclear magnetic resonance (NMR) spectra of silica-supported $Os_3(^{13}CO)_{12}$ samples prepared in several different ways. Our results yield both the isotropic chemical shift and the principal components of the chemical shift tensor for each carbonyl resonance. Spectra have been assigned by comparison to solution NMR spectra of a variety of osmium carbonyl clusters that are models for the proposed surface-attached structures: $HOs_3(CO)_{10}(OR)$ (R = CH_3, C_6H_5, $SiEt_3$), $HOs_3(CO)_{10}(O_2CH)$, $Os_3(CO)_{10}(OCH_3)_2$, and $[Os(CO)_3Cl_2]_2$. Spectra of samples prepared by impregnation of silica with a solution of $Os_3(^{13}CO)_{12}$ provide evidence for a physisorbed $Os_3(CO)_{12}$ species undergoing fast isotropic motion. For samples prepared by refluxing $Os_3(^{13}CO)_{12}$ and SiO_2 in *n*-octane, a spectrum containing five distinct resonances is observed, consistent with a $HOs_3(CO)_{10}(OSi{\equiv})$ species having C_s symmetry. The chemical shift anisotropy parameters measured for these resonances at 20 °C suggest that this species is undergoing rapid (≫32 kHz) large-angle (90–120°) rotational jumps. Spectra of samples prepared by vacuum pyrolysis (200 °C) are consistent with Os(II) carbonyl species that are immobile on the 10^{-5}–10^{-4}-s time scale. These results demonstrate the utility of ^{13}C NMR spectroscopy for studying the structures and dynamics of supported metal carbonyl clusters.

Supported metal complexes have been widely investigated both as novel catalysts and as models for the supported metal crystallites that are commonly used as catalysts in petroleum refining.[1-5] In contrast to supported metal crystallites, supported metal complexes may provide uniform catalytic centers which are more readily analyzed, thus allowing the identification of important catalyst properties through systematic synthesis and characterization.[3,5] However, determining the detailed structures of supported complexes has proven to be a challenging task, and a wide array of techniques have been applied to the problem.[3,6] While vibrational spectroscopies (infrared, Raman, and inelastic electron tunneling) have been most widely used to date, there has been a growing interest in the use of extended X-ray absorption fine structure (EXAFS)[7,8] and magic-angle-spinning nuclear magnetic resonance (MAS NMR) spectroscopies.[9] Despite the well-known utility of ^{13}C NMR spectroscopy for characterizing metal complexes in solution, ^{13}C NMR spectroscopy has not yet been widely exploited to study supported metal complexes. This may be, in part, because special techniques must often be used. Isotopic enrichment is frequently required to obtain useful signal-to-noise ratios in a reasonable period of time, and magic-angle spinning and high-power proton decoupling are generally necessary to obtain high resolution. Many samples also require the use of sealed sample holders to prevent contact with air.[9-11] Despite these compli-

---

(1) Yermakov, Yu. I.; Kuznetsov, B. N.; Zakharov, V. A. *Catalysis by Supported Complexes*; Elsevier: Amsterdam, 1981.

(2) Bailey, D. C.; Langer, S. H. *Chem. Rev.* **1981**, *81*, 109.

(3) Hartley, F. R. *Supported Metal Complexes*; Reidel: Dordrecht, Holland, 1985.

(4) Gates, B. C. In *Metal Clusters*; Moskovits, M., Ed.; Wiley: New York, 1986; p 283.

(5) Basset, J. M.; Choplin, A. *J. Mol. Catal.* **1983**, *21*, 95.

(6) Gates, B. C.; Lieto, J. *CHEMTECH* **1980**, *10*, 248.

(7) Evans, J. *Spectrochim. Acta* **1987**, *43A*, 1511.

(8) Duivenvoorden, F. B. M.; Koningsberger, D. C.; Uh, Y. S.; Gates, B. C. *J. Am. Chem. Soc.* **1986**, *108*, 6254.

(9) (a) Fischer, A. B.; Bruce, J. A.; McKay, D. R.; Maciel, G. E.; Wrighton, M. S. *Inorg. Chem.* **1982**, *21*, 1766. (b) Hanson, B. E.; Wagner, G. W.; Davis, R. J.; Motell, E. *Inorg. Chem.* **1984**, *23*, 1635. (c) Liu, D. K.; Wrighton, M. S.; McKay, D. R.; Maciel, G. E. *Inorg. Chem.* **1984**, *23*, 212. (d) McKenna, W. P.; Eyring, E. M. *J. Mol. Catal.* **1985**, *29*, 363. (e) Komoroski, R. A.; Magistro, A. J.; Nicholas, P. P. *Inorg. Chem.* **1986**, *25*, 3917. (f) Prigano, A. L.; Trogler, W. C. *J. Am. Chem. Soc.* **1987**, *109*, 3586. (g) Hedden, D.; Marks, T. J. *J. Am. Chem. Soc.* **1988**, *110*, 1647. (h) Dahmen, K.-H.; Hedden, D.; Burwell, R. L.; Marks, T. J. *Langmuir* **1988**, *4*, 1212. (i) Weiss, K.; Lossel, G. *Angew. Chem., Int. Ed. Engl.* **1989**, *28*, 62.

0020-1669/91/1330-4732$02.50/0